

H4.SMR/1519-4

**"Seventh Workshop on Non-Linear Dynamics and
Earthquake Prediction"**

29 September - 11 October 2003

**Stress & Seismicity in Areas of Relic Descending
Lithospheric slabs: The South Eastern Carpathians**

Alik T. Ismail-Zadeh

**International Institute of Earthquake Prediction Theory
and Mathematical Geophysics, Russian Academy of Sciences
Moscow, Russia**

**Now at: Institute of Geophysics, University of Karlsruhe
Karlsruhe, Germany
e-mail: Ismail-Zadeh@gpi.uni-karlsruhe.de**

United Nations Educational Scientific and Cultural Organization
and
International Atomic Energy Agency

THE ABDUS SALAM
INTERNATIONAL CENTRE FOR THEORETICAL PHYSICS

Seventh Workshop
“Non-Linear Dynamics and Earthquake Prediction”
29 September to 12 October 2003

**STRESS AND SEISMICITY IN AREAS OF
RELIC DESCENDING LITHOSPHERIC SLABS:
THE SOUTHEASTERN CARPATHIANS**

Alik T. Ismail-Zadeh

International Institute of Earthquake Prediction Theory and
Mathematical Geophysics, Russian Academy of Sciences,
Warshavskoye shosse 79-2, Moscow 113556, Russia.
E-mail: aismail@mitp.ru

Now at: Geophysical Institute, University of Karlsruhe,
Hertzstr. 16, Karlsruhe 76187, Germany.
E-mail: Alik.Ismail-Zadeh@gpi.uni-karlsruhe.de

MIRAMARE-TRIESTE

September 2003

Modelling of descending slab evolution beneath the SE-Carpathians: implications for seismicity

A. Ismail-Zadeh¹, B.Müller, and F. Wenzel

Geophysikalisches Institut, Universität Karlsruhe, Germany

Abstract - Recent findings from regional seismic tomography and refraction studies and from GPS studies on vertical movements together with extremely high intermediate-depth seismicity in the Vrancea region (Romania) point towards the interpretation that the lithospheric slab, descending beneath the SE-Carpathians, approaches a stage of break-off or even it is already delaminated from the crust. To understand processes of stress generation due to the descending slab, we analyse tectonic stress, induced by the slab sinking in the mantle, by means of analytical and numerical modelling. We find that the maximum shear stress migrates from the upper surface of the slab to its lower surface in the course of changes in slab dynamics from its active subduction through roll-back movements to sinking solely due to gravity. The changes in stress distribution can explain the location of hypocentres of Vrancea events at the side of the slab adjacent to the Eastern European craton. To analyse a process of slab delamination, we develop a two-dimensional thermomechanical finite-element model of a slab sinking in the mantle due to gravity and overlain by the continental crust. The model predicts lateral compression in the slab as inferred from the stress axes of earthquakes and its thinning and necking. The maximum stress occurs in the depth range of 80 km to 200 km, and the minimum stress falls into the depth range of 40 km to 80 km. The area of maximum shear stress coincides with the region of high seismicity, and minimum shear stress in the model is associated with the lower viscosity zone. Uplift of the crust starts before the slab detachment. Just after the detachment the tectonic stress in the slab is still high enough to lead to a seismic activity, and the stress decreases significantly in several million years.

1. Introduction: Vrancea Seismicity and Geodynamics

Repeated intermediate-depth large earthquakes of the SE-Carpathians (Vrancea) cause destructions in Bucharest and shake the central and eastern European cities at distances of several hundred kilometres away from the hypocentres of the events. The earthquake-prone Vrancea region is situated at the bend of the

¹ On leave from the International Institute of Earthquake Prediction Theory and Mathematical Geophysics, Russian Academy of Sciences, Moscow.

SE-Carpathians and bounded on the north and north-east by the Eastern European craton (EEC), on the east and south by the Moesian platform (MP), and on the west by the Transylvanian basin (TB).

The epicentres of mantle earthquakes in the Vrancea region are concentrated within a very small area (Fig. 1), and the distribution of the epicentres is much denser than that of intermediate-depth events in other intracontinental regions. The projection of the foci on the NW-SE vertical plane across the bend of the Eastern Carpathians (section AB in Fig.1) shows a seismogenic volume about 100 km long, about 40 km wide, and extending to a depth of about 180 km. The body is interpreted as a lithospheric slab descending in the mantle. Beyond this depth the seismicity ends suddenly: a seismic event beneath 180 km represents an exception. A seismic gap at depths of 40-70 km led to the assumption that the lithospheric slab was already detached. According to the historical catalogue of Vrancea events, large intermediate-depth shocks with magnitudes $M_W > 6.5$ occur three to five times per century. In the XXth century, large events at depths of 70 to 170 km occurred in 1940 with moment magnitude $M_W = 7.7$, in 1977 $M_W = 7.4$, in 1986 $M_W = 7.1$, and in 1990 $M_W = 6.9$ (Onicescu and Bonjer 1997).

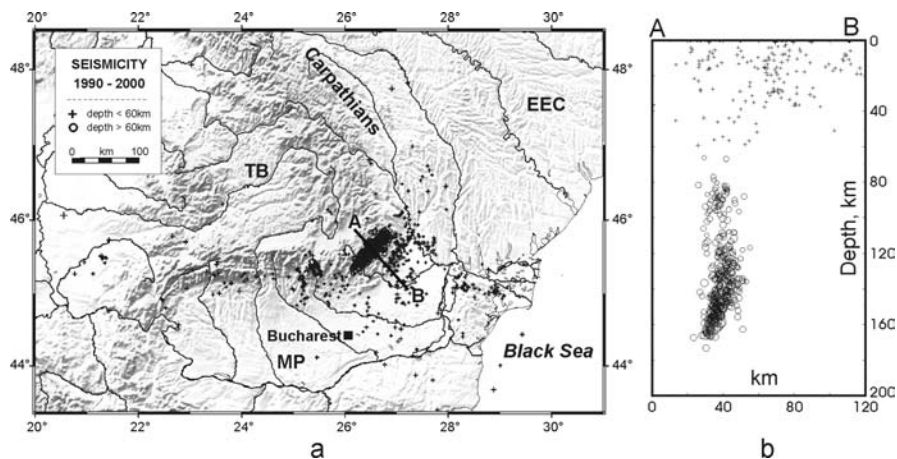


Fig. 1. Location map of observed seismicity in Romania with magnitude $M_W \geq 3$ (after Sperner et al. 2001). (a) Epicentres of Vrancea earthquakes. (b) Hypocentres of the same earthquakes projected onto the vertical plane AB along the NW-SE direction. TB, Transylvanian basin; EEC, Eastern European craton; MP, Moesian platform.

The 1940 earthquake gave rise for the development of a number of geodynamic models for this region. Gutenberg and Richter (1954) drew attention to the Vrancea region as a place of remarkable intermediate depth seismicity. Later McKenzie (1972) suggested this seismicity to be associated with a relic slab sinking in the mantle and now overlain by continental crust. The 1977 disastrous earthquake and later the 1986 and 1990 earthquakes brought again up the discussion about the nature of the earthquakes. The Vrancea region was considered

(Fuchs et al. 1979) as a place where the sinking slab was already detached from the continental crust. Oncescu (1984) proposed that the intermediate-depth events are generated in a zone that separates the sinking slab from the neighbouring immobile part of the lithosphere rather than in the sinking slab itself. Linzer (1996) explained the nearly vertical position of the Vrancea slab as the final rollback stage of a small fragment of oceanic lithosphere. Gibracea and Frisch (1998) assumed that the break-off, affecting only the crustal portion of the slab, was followed by the horizontal delamination of its lower portion. Sperner et al. (2001) suggested a model of Miocene subduction of oceanic lithosphere beneath the Carpathian arc and subsequent gentle continental collision, which transported cold and dense lithospheric material into the mantle. Recent investigations within the framework of the SFB 461 (Collaborative Research Centre: Strong Earthquakes) resulted in modern data sets from seismic refraction techniques, tomography, and geodesy which led to a refinement of the geodynamic model of the Vrancea region (Sperner, this volume).

The active subduction ceased about 10 Ma ago (Wenzel et al. 1998). Subsequently, the initial flat subduction began to steepen to its present-day nearly vertical orientation. Now the cold slab (hence denser than the surrounding mantle) beneath the Vrancea region sinks due to gravity. The hydrostatic buoyancy forces help the slab to subduct, but viscous and frictional forces resist the descent. At intermediate depths these forces produce an internal stress, and earthquakes occur in response to this stress. Ismail-Zadeh et al. (2000) showed that the maximum shear stress in a descending slab accumulates in the depth range of 70 km to 160 km in a very narrow area and the depth distribution of the annual average seismic energy released in earthquakes has a shape similar to that of the depth distribution of the stress magnitude in the slab.

One question to be addressed in this paper concentrates on the pattern of earthquake hypocentres within the slab. Seismic tomographic studies revealed a body of high *P*-wave velocities beneath the Vrancea region, which was interpreted as a slab descending in the mantle (Wenzel et al. 1998a,b; Bijwaard and Spakman 2000). Its dimensions exceed the seismogenic volume by far.

In 1999 an international tomographic experiment with 120 seismic stations was realised in SE-Romania (Martin et al. 2001). During the field experiment 160 local events with magnitude $M_l \geq 2.0$ and 450 teleseismic events with magnitude $M_b \geq 5.0$ were recorded. The station distance ranged from 15-20 km (the Vrancea region) to 25-30 km (outer margins of the network) covering a region of about 350 km in diameter. First preliminary results were achieved through an inversion of the teleseismic data. Data inversion reveals a high-velocity body with maximum *P*-wave velocity perturbations of +3.5% in comparison with the background model (see Fig. 2). This high-velocity body is interpreted as the descending lithospheric slab. It reaches a depth of at least 350 km which is in good agreement with results of previous low-resolution seismic tomography studies (e.g., Wortel and Spakman 2000).

The high-resolution seismic tomographic image of the body (Fig. 2; Martin et al. 2001) shows that Vrancea intermediate-depth earthquakes are located at the opposite side of the slab (or lower surface of the descending slab) as compared to

zones of active subduction, where seismicity is associated with the upper surface of subducting lithosphere.

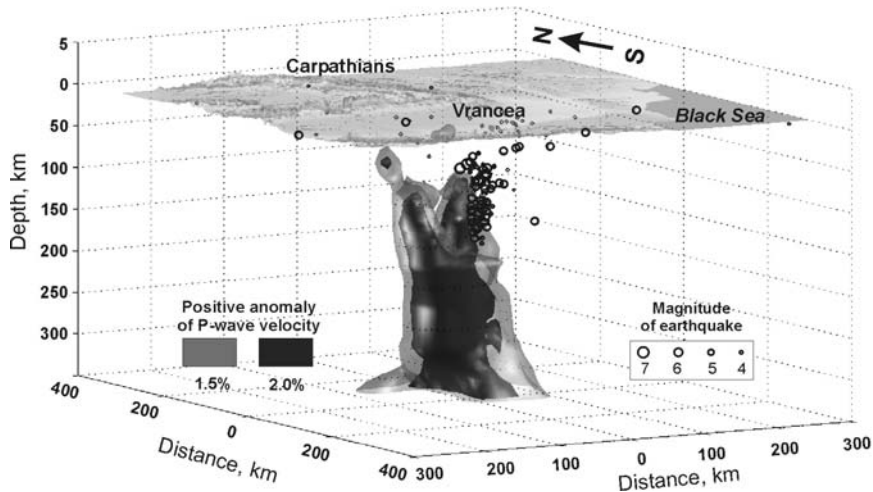


Fig. 2. Seismic tomographic image of the Vrancea slab and hypocentres of intermediate-depth seismicity (based on Martin et al. 2001).

Another question is whether the Vrancea slab is still attached to the crust or has been already detached. At the present time the upper limit of the high-velocity body cannot be defined even from the high-resolution seismic tomography. Further information on its upper limit comes from the model based on seismic refraction data: about 10 km high low-velocity zone is detected at a depth of about 50 km beneath the Vrancea region (Hauser et al. 2001). This zone coincides with the seismic gap at same depths and can be interpreted as a zone of weakened mantle (or lower crustal) material.

A GPS network operates in the SE-Carpathians since 1997. Recent geodetic measurement revealed relative uplift rates of at least 10 mm a^{-1} (mean uplift rate of 22 mm a^{-1} with an average confidence range of 13.4 mm a^{-1}) in the Vrancea region (Dinter et al. 2001). A possible explanation of the uplift is that the descending slab is decoupled (or still decoupling) from the overlying crust. Hence the load of the slab decreases, and as a result the released crust starts to uplift.

A principal objective of this contribution is to understand the process of stress generation beneath the Vrancea region by means of analytical and numerical models. We analyse the evolution of shear stress induced by the descending slab from active subduction of the lithosphere to its sinking only due to gravity forces. An analytical model of corner flow (Batchelor 1967) is used to explain different patterns of seismicity during the slab sinking. Also we use two-dimensional numerical model of a descending slab to study the stress distribution during the process of slab sinking and delamination.

2. Shear stress evolution induced by the descending Vrancea slab – a corner flow model

In this section we consider a simple fluid dynamical model which provides an explanation for the observed distribution of seismicity in the Vrancea region. The Vrancea slab, which is believed to sink beneath the SE-Carpathian arc, separates the mantle into two portions (or two corner sub-domains). Considering that stresses released in earthquakes are related to the level of shear stress, we calculate shear stress distributions in the each corner sub-domain by using an analytical model for corner flow (Batchelor 1967). McKenzie (1969) used the corner flow model to study subduction zone dynamics and causes of plate motions. Later Stevenson and Turner (1977) and Tovish et al. (1978) used the same model to investigate the torque balance on the slab and angle of subduction for Newtonian and non-Newtonian rheologies of the mantle.

The descending slab must induce stresses within the surrounding mantle. Its motion will therefore influence the flow of the mantle. The principal forces determining the motion are the normal forces on the upper and lower surfaces of the slab (due to pressure variations in the surrounding mantle), gravity and resistance forces. Although the latter forces can contribute to the estimation of shear stresses on the slab, we follow McKenzie (1969) and Tovish et al. (1978) and omit resistance forces from the consideration to analyse viscous stresses only. Body forces caused by lateral thermal (density) variations are neglected, because our analytical model is purely mechanical (no thermal effects are considered in this section). Another assumption of the model is that flow in the mantle is governed by a viscous constitutional relationship, although it was shown that the shear stresses on the slab are reduced insignificantly, if the mantle behaves as non-Newtonian fluid (Tovish et al. 1978). Thus several of these assumptions are unlikely to be valid for mantle flow, but they enable analytical solutions to be obtained.

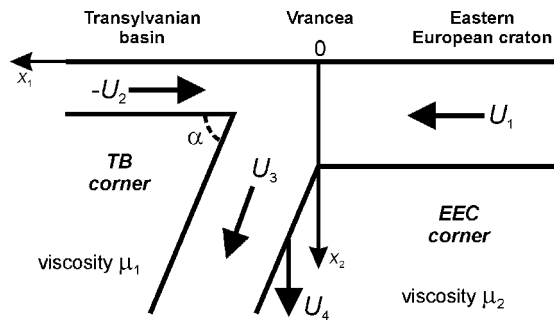


Fig. 3. Geometry and applied velocities of the model of corner flow induced by the descending slab beneath the Vrancea region.

The corner flows are assumed to be two-dimensional. Figure 3 illustrates how the descending slab divides the mantle into two corners where flows are induced

by the motion of the slab. We locate the Vrancea region at the origin of co-ordinates $x_1=0$, $x_2=0$. Axes Ox_1 and Ox_2 are directed leftward and downward, respectively. Surfaces $x_2=0$, $x_1<0$ and $x_2=0$, $x_1\geq 0$ move towards the trench ($x_1=0$) with constant velocity U_1 and $-U_2$, respectively. The descending slab extends from the origin of co-ordinates downward at the dip angle α to the positive x_1 axis. The slab moves with constant velocity U_3 and/or vertical velocity U_4 (due to gravity). The model slab divides the viscous flow into two corners: “Transylvanian basin” corner (TB corner) and “East-European craton” corner (EEC corner). The applied velocities induce a viscous flow, and the flow and tectonic shear stress are determined within the two corners.

The velocity components (v_1 , v_2) of the mantle flow and maximum tectonic (deviatoric) shear stress τ_{\max} in each corner can be found from the following expressions (Turcotte and Schubert 2002; Eqs. 6-110 and 6-111)

$$v_1 = -(A_i x_1 + B_i x_2) \frac{x_1}{x_1^2 + x_2^2} - B_i \arctan \frac{x_2}{x_1} - D_i, \quad (1)$$

$$v_2 = -(A_i x_1 + B_i x_2) \frac{x_2}{x_1^2 + x_2^2} + A_i \arctan \frac{x_2}{x_1} + C_i, \quad (2)$$

$$\tau_{\max} = 2\mu_i \frac{|A_i x_2 - B_i x_1|}{x_1^2 + x_2^2}, \quad (3)$$

where A_i , B_i , C_i , and D_i are constants, and $i=1$ and $i=2$ correspond to TB and EEC corners, respectively. Their values are determined by boundary conditions.

The viscosity of cooled mantle material beneath the old EEC ($\mu_2=10^{21}$ Pa s) is assumed to be only five times higher than that of the mantle beneath the young TB ($\mu_1=2\times 10^{20}$ Pa s). High mantle temperature and fluids beneath the TB may decrease the viscosity drastically, and hence the ratio between the mantle viscosities beneath the EEC and TB would be even larger.

The boundary conditions for the TB corner are $v_1 = -U_2$, $v_2 = 0$ at $x_2 = 0$, $x_1 > 0$ (or $\arctan(x_2/x_1) = 0$) and $v_1 = U_3 \cos \alpha$, $v_2 = U_3 \sin \alpha + U_4$ at $x_2 = x_1 \tan \alpha$ (or $\arctan(x_2/x_1) = \alpha$). An application of these boundary conditions to the equations for velocity leads to the following expressions for constants A_1 , B_1 , C_1 , and D_1 :

$$A_1 = \frac{-U_2 \sin^2 \alpha + U_3 \alpha \sin \alpha + U_4 (\alpha + \sin \alpha \cos \alpha)}{\alpha^2 - \sin^2 \alpha}, \quad (4)$$

$$B_1 = \frac{-U_2 (\alpha - \sin \alpha \cos \alpha) - U_3 (\alpha \cos \alpha - \sin \alpha) + U_4 \sin^2 \alpha}{\alpha^2 - \sin^2 \alpha}, \quad (5)$$

$$C_1 = 0, \quad D_1 = -A_1 + U_2. \quad (6)$$

The boundary conditions for the EEC corner are $v_1 = U_1$, $v_2 = 0$ at $x_2 = 0$, $x_1 < 0$ (or $\arctan(x_2/x_1) = \pi$) and $v_1 = U_3 \cos \alpha$, $v_2 = U_3 \sin \alpha + U_4$ at $x_2 = x_1 \tan \alpha$ (or $\arctan(x_2/x_1) = \alpha$). Substituting the boundary conditions into the equations for velocity, we obtain the following expressions for constants A_2 , B_2 , C_2 , and D_2 :

$$A_2 = \frac{U_1 \sin^2 \alpha - U_3 (\pi - \alpha) \sin \alpha - U_4 (\pi - \alpha - \sin \alpha \cos \alpha)}{(\pi - \alpha)^2 - \sin^2 \alpha}, \quad (7)$$

$$B_2 = \frac{-U_1 (\pi - \alpha + \sin \alpha \cos \alpha) - U_3 (\cos \alpha (\pi - \alpha) + \sin \alpha) + U_4 \sin^2 \alpha}{(\pi - \alpha)^2 - \sin^2 \alpha}, \quad (8)$$

$$C_2 = -\pi A_2, \quad D_2 = -A_2 - \pi B_2 - U_1. \quad (9)$$

We consider three subsequent phases of the evolution of the descending lithosphere beneath the Vrancea: (i) active subduction ($\alpha=30^\circ$, $U_1=U_3=5 \text{ cm yr}^{-1}$); (ii) slab steepening due to gravity and slab roll-back ($\alpha=60^\circ$, $U_2=U_4=5 \text{ cm yr}^{-1}$); and (iii) gravity-driven slab sinking ($\alpha=85^\circ$, $U_4=5 \text{ cm yr}^{-1}$). Figure 4 shows the flow field and contours of constant shear stress for the model.

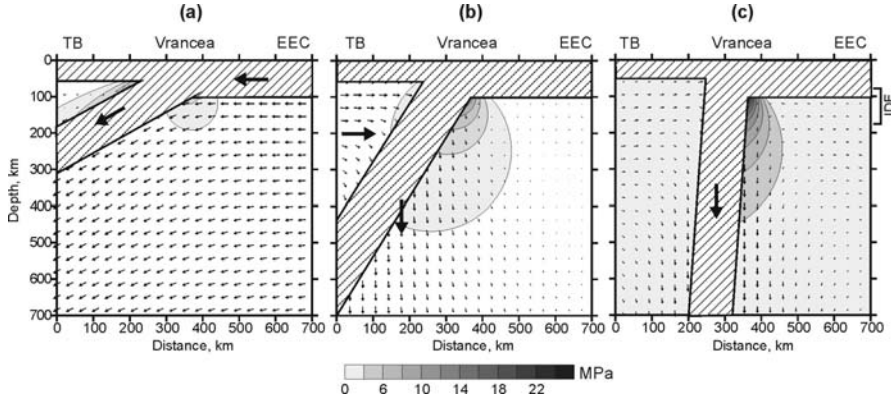


Fig. 4. Modelled tectonic shear stress and flow in the mantle induced by a slab descending beneath the Vrancea region for three phases of slab evolution: (a) active subduction, (b) slab steepening, and (c) slab sinking only due to gravity. Flow is indicated by the arrows, the shading represents the magnitudes of the shear stresses. IDE, intermediate-depth earthquakes.

According to Sperner et al. (2001) the dip angle of the Vrancea subduction in Miocene times was about 25° . Fig. 4,a illustrates the pattern of mantle flow and distribution of stress during the active subduction of the Vrancea lithosphere. The pattern of the flow and shear stresses coincide with that of the McKenzie model (1969). Namely, the maximum shear stresses are concentrated at the upper surface

of the descending slab. The model predictions are in good agreement with the locations of hypocentres of earthquakes within the so-called Wadati-Benioff zones associated with the active subduction in other seismic belts (e.g., Zhao 2001).

When the active subduction beneath the SE-Carpathians terminated, a rollback movement of the slab resulted in a redistribution of shear stress in the mantle. The maximum shear stresses are shifted from the upper to lower surface of the slab due to changes in the applied velocities (Fig.4,b). This effect is amplified during the final phase of slab evolution when the lithospheric plate sinks into the mantle driven only by gravity (Fig.4,c). According to Eq. (3), the higher the mantle viscosity beneath the EEC, the greater the magnitude of shear stress at the corner. The area of the maximum shear stresses in the model roughly coincides with the depth range of intermediate-depth events (IDE in Fig. 4) in SE-Carpathians. Ismail-Zadeh et al. (1999) showed that large earthquakes, generated by a dynamic model of a rigid slab descending in the viscoelastic mantle, are also concentrated at the lower surface of the Vrancea slab, but not at its upper surface.

Although our model presented here is based on simplified assumptions, it illustrates how changes in the dynamics of the descending slab result in a significant redistribution of shear stresses and hence in spatial changes of seismicity.

3. Past, present and future of the Vrancea slab inferred from numerical models

In this section we present two-dimensional numerical models of the slab evolution. We compute the flow and tectonic stresses induced by the descending slab during the processes of slab delamination and full detachment of the slab from the crust.

3.1. Model description

In the numerical models the mantle is at rest before the onset of slab descend, thus convectively neutral. The motion is only caused by the descending slab. The initial geometry and boundary conditions for the models are shown in Fig. 5. A viscous incompressible fluid with variable density and viscosity fills the model region $0 \leq x \leq L$, $-H \leq z \leq h$ divided into five sub-domains by material interfaces: atmosphere above the surface, upper crust, lower crust, slab, and mantle. The density ρ and viscosity μ are constant within each, the upper and lower crust and mantle. The topography line approximates a free surface, because the density of the upper layer (the atmosphere) equals zero, and the viscosity is sufficiently low compared to that in the crust. The slab is modelled as being denser than the surrounding mantle, and therefore tends to sink gravitationally. The density and viscosity of the slab depend on the temperature T . Since we concentrate on an analysis of stresses induced by the sinking slab, the heat transfer in the mantle is neglected, although we understand its importance in general models of mantle convection.

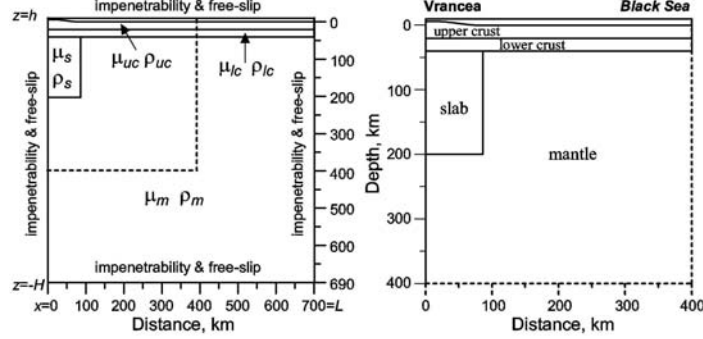


Fig. 5. Geometry of the model region with boundary conditions as indicated. The right panel presents an enlarged view of the model sub-region marked in the left panel by a dashed line.

We tested our models with respect to the stability of the results to variations of the density contrast, viscosity ratio between the slab and the surrounding mantle, and geometry of the slab. We considered (1) a density contrast ranging from 30 to 100 kg m⁻³; (2) several values of the viscosity ratio: 10, 100, and 500, using a fixed density contrast of 70 kg m⁻³; and (3) a variation of the initial depth of the slab penetration into the mantle ranging from 150 to 400 km. The model results show their robustness to these variations.

We solve the equation of motion (the Stokes equation) in terms of the stream function

$$4 \frac{\partial^2}{\partial x \partial z} \mu(x, z) \frac{\partial^2 \psi}{\partial x \partial z} + \left(\frac{\partial^2}{\partial z^2} - \frac{\partial^2}{\partial x^2} \right) \mu(x, z) \left(\frac{\partial^2 \psi}{\partial z^2} - \frac{\partial^2 \psi}{\partial x^2} \right) = -g \frac{\partial \rho(x, z)}{\partial x}, \quad (10)$$

where $x=x_1$ and $z=x_2$. We assume impenetrability (no flow out of and into the model region) and free-slip boundary conditions, considering external forces to be negligible:

$$\psi = \partial^2 \psi / \partial x^2 = 0 \quad \text{at } x=0 \text{ and } x=L, \quad (11)$$

$$\psi = \partial^2 \psi / \partial z^2 = 0 \quad \text{at } z=-H \text{ and } x=h.$$

Temperature within the slab is calculated from the following equation (McKenzie 1969):

$$\frac{T(x, z)}{T^*} = 1 - \frac{2}{\pi} \exp \left[- \left(\frac{\rho_s c_p l}{2\kappa} \frac{\partial \psi}{\partial x} + \left[\left(\frac{\rho_s c_p l}{2\kappa} \frac{\partial \psi}{\partial x} \right)^2 + \pi^2 \right]^{1/2} \right) \frac{z}{H} \right] \sin \frac{\pi x}{L}, \quad (12)$$

where T^* is the temperature of the mantle surrounding the slab, ρ_s is the initial density of the slab, c_p is the specific heat at constant pressure, l is the slab thickness, and κ is the thermal conductivity of the slab.

The temperature-dependent density and viscosity of the slab are found from the following equations:

$$\rho(T) = \rho_s [1 - \alpha_T (T - T_0)], \quad \mu(T) = \mu_s \exp\left(\frac{E}{RT} - \frac{E}{RT_0}\right), \quad (13)$$

where μ_s is the initial viscosity of the slab, T_0 is temperature at the bottom of the crust, α_T is volumetric coefficient of thermal expansion, E is the activation energy, and R is the universal gas constant. The positions of the material interfaces as functions of time are governed by the following differential equations:

$$\frac{dX}{dt} = \frac{\partial \psi}{\partial z}, \quad \frac{dZ}{dt} = -\frac{\partial \psi}{\partial x}, \quad (14)$$

where the points (X, Z) are on the initial interfaces at $t=0$. The initial distributions ($t=0$) of density and viscosity and the positions of the material interfaces are known.

The maximum tectonic shear stress τ_{\max} is given by

$$\tau_{\max} = \left[\frac{1}{2} (\tau_{xx}^2 + \tau_{zz}^2 + 2\tau_{xz}^2) \right]^{1/2} = \mu \left[4 \left(\frac{\partial^2 \psi}{\partial x \partial z} \right)^2 + \left(\frac{\partial^2 \psi}{\partial z^2} - \frac{\partial^2 \psi}{\partial x^2} \right)^2 \right]^{1/2}, \quad (15)$$

where τ_{ij} ($i, j = x, z$) are the components of the tectonic (deviatoric) stress tensor.

To solve the equations, that is, to compute the dependence of velocity, slab temperature, material interfaces, and shear stress on time, we employ the Galerkin method and finite element codes developed by Naimark et al. (1998). The model region is divided into rectangular 98×94 elements in the x and z directions.

We use dimensionless variables, whereas in presenting the results for stress and velocity we scale them as follows: the time scale t^* , the velocity scale v^* , and the stress scale σ^* are taken respectively as $t^* = \mu^* / [\rho^* g(H+h)]$, $v^* = \rho^* g(H+h)^2 / \mu^*$, and $\sigma^* = \rho^* g(H+h)$, where μ^* and ρ^* are the typical values of mantle viscosity and density. The parameter values used in the modelling are listed in Table 1.

The viscosity being a least-known physical parameter is the only tuning parameter in our numerical models. We choose the value of typical viscosity μ^* , entering into the scaling relationships for t^* and v^* , so that the times of descending slab evolution predicted by the models are close to realistic geological times. The viscosity of the model mantle is chosen to be in agreement with the average viscosity for the upper mantle (long-dashed curve in Fig. 2, Forte and Mitrovica

2001). The densities of the upper and lower crust in the model are the averaged densities converted from P-wave velocities (Hauser et al. 2001).

Table 1. Model parameters

Notation	Meaning	Value
c_p	specific heat at constant pressure, $\text{J kg}^{-1} \text{K}^{-1}$	1000 (1)
E	activation energy per mole, kJ mol^{-1}	2 (1)
g	acceleration due to gravity, m s^{-2}	9.8
h	height above the surface, km	5
$H+h$	vertical size of the model, km	700
l	thickness of the slab, km	90
L	horizontal size of the model, km	700
R	universal gas constant, $\text{J mol}^{-1} \text{K}^{-1}$	8.3 (1)
t^*	time scale, yr	14
v^*	velocity scale, m yr^{-1}	5×10^4
T_0	temperature at the bottom of the lower crust, K	873 (2)
T^*	temperature of the mantle, K	1573 (2)
α_T	volumetric coefficient of thermal expansion, K^{-1}	3×10^{-5} (1)
κ	coefficient of thermal conductivity, $\text{W m}^{-1} \text{K}^{-1}$	4 (1)
μ^*	typical value of viscosity, Pa s	10^{19}
μ_{uc}	effective viscosity of the upper crust, Pa s	3×10^{20}
μ_{lc}	viscosity of the lower crust, Pa s	5×10^{19}
μ_m	viscosity of the mantle, Pa s	3×10^{20}
μ_s	initial viscosity of the slab, Pa s	10^{21}
ρ^*	typical value of density, kg m^{-3}	3.37×10^3
ρ_{uc}	density of the upper crust, kg m^{-3}	2.76×10^3
ρ_{lc}	density of the lower crust, kg m^{-3}	2.97×10^3
ρ_m	density of the mantle, kg m^{-3}	3.3×10^3
ρ_s	initial density of the slab, kg m^{-3}	3.37×10^3
σ^*	stress scale, Pa	2.36×10^{10}

(1) Turcotte and Schubert 2002; (2) Demetrescu and Andreescu 1994

3.2. Evolution of the descending slab from the Late Miocene to the present

In the numerical model we assume that the initial thickness of the crust is 40 km, and the slab penetrates into the mantle to the depth of 200 km. The position of the model slab approximates the location of the slab at the end of Miocene times. Figure 6 presents the model evolution of the descending slab from 6.7 Ma ago to the present day. To enhance a visualisation of the numerical results, we present a portion of the model limited to the depth and width of 400 km.

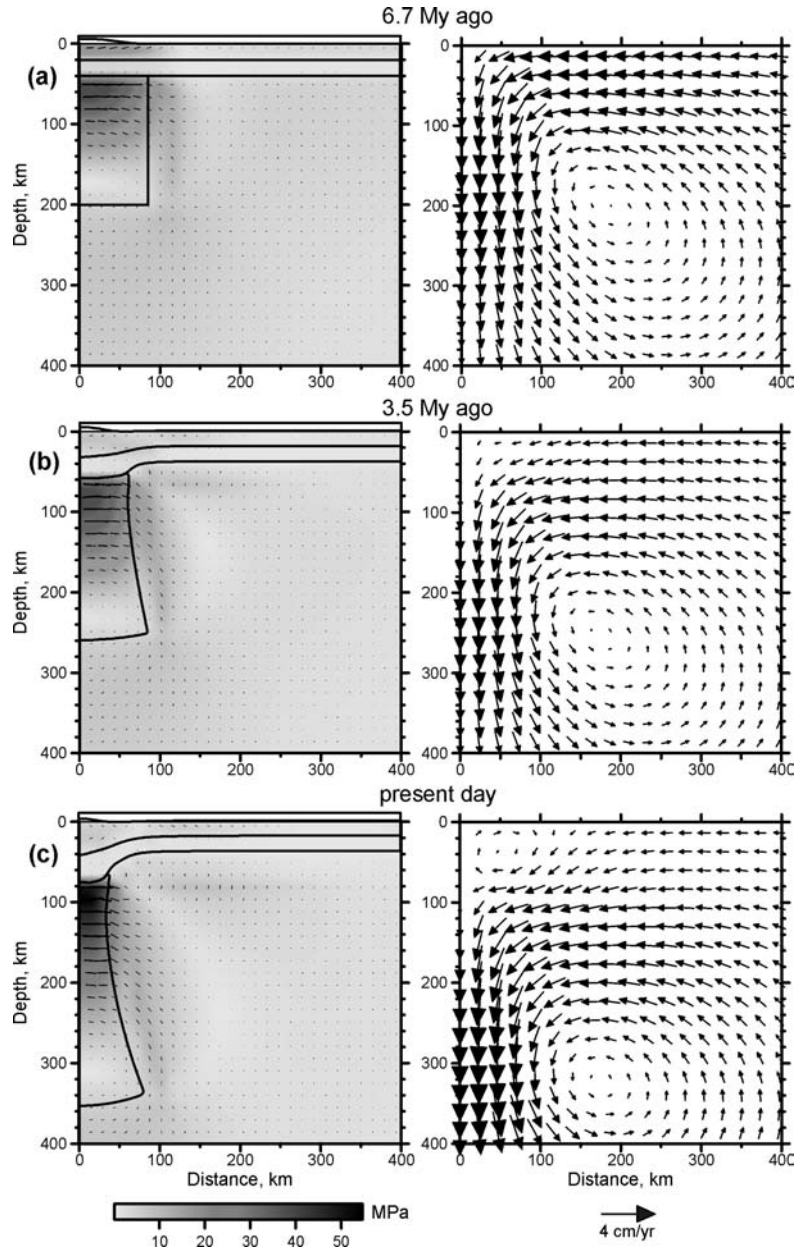


Fig. 6. Maximum tectonic shear stresses and axes of compression (left panel) and flow field (right panel) for the model evolution of the Vrancea slab (attached to the crust) descending in the mantle at successive times indicated in (a)-(c).

At the early stage of the descending slab evolution (6.7 Ma ago) maximum shear stresses are high in the upper portion of the slab (~ 30 MPa) and in the upper crust (~ 20 MPa) and low (~ 10 MPa) in the lower crust and mantle (Fig. 6a, left panel). The stress decreases within the crust during the time between 6.7 Ma and 3.5 Ma, while it increases within the upper portion of the slab (Fig. 6b). Until present the model slab penetrates the mantle to the depth of about 350 km, and high maximum tectonic shear stresses (~ 35 to 55 MPa) are predicted at a depth range of about 80 to 180 km (Fig. 6c).

We consider this stage of the slab evolution to be related to the present-day situation in Vrancea, because (i) large seismic events are located at the same depths where our model predicts high shear stresses and (ii) a high velocity body beneath the Vrancea region is observed down to depths of 350 km (Wortel and Spakman 2000; Martin et al. 2001). A zone of low shear stress in the modelled lower crust (< 10 MPa) is associated with the zone of low seismicity and observed zone of low seismic wave velocity shallower than 55 km (Hauser et al. 2001). Shear stresses decrease with depth within the slab as a result of temperature increase with depth.

Figure 6 (left panel) illustrates also the axes of maximum deviatoric compression. The axes of tension are perpendicular to the axes of compression. The axes of compression are subhorizontal in the upper portion of the slab (Fig. 6c) being in a good agreement with observations. Using numerous fault-plane solutions for intermediate-depth shocks, Oncescu and Trifu (1987) show that the compressional axes are almost horizontal and directed NW-SE.

The mantle flow induced by the descending slab is presented in Fig. 6 (right panel). Initially the motion of the crustal and uppermost mantle material is directed downward. The mantle flow is driven continuously by the descending slab (maximum rate of slab descent in Fig. 6c is about 4 cm yr^{-1}), whereas the upper crust subducted to the depths of about 40 km starts to rebound isostatically (uplift rate in the crust is about 0.5 cm yr^{-1}).

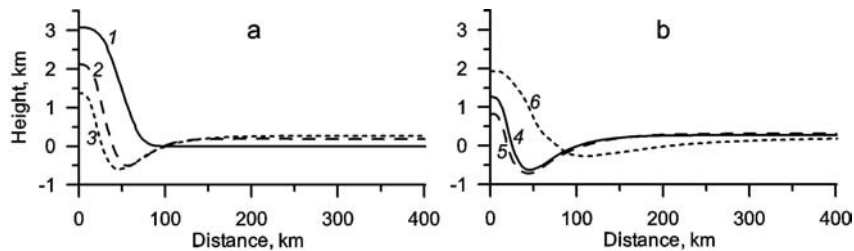


Fig. 7. Surface topography predicted by the numerical models of (a) attached and (b) detached Vrancea slab: Curves: 1, 6.7 Ma ago (initial position of the model surface topography); 2, 3.5 Ma ago; 3, at present-day; 4, in 0.5 Ma after slab detachment; 5, in 2.0 Ma; and 6, in 8.5 Ma.

The shape of the slab is controlled by the circulation of mantle material. The slab becomes thinner at the shallow levels (100-140 km) and thicker below (300-

350 km), while the crust thickens above the slab due to flow of the crustal material induced by the descending slab. The motion results in changes of the surface topography contributing to the evolution of Carpathians and foredeep basin development. (Fig. 7a). An initial maximum elevation of the Carpathian mountains was prescribed to be about 3 km (curve 1, Fig. 7a). As the Vrancea slab sinks (curve 2 and 3), a significant basin developed in the foredeep area and the maximum height of the Carpathians decreased to the today observed level of ca. 1.5 km (curve 3).

3.3. Evolution of the descending slab after slab break-off

To study the evolution of shear stress after slab break-off, we develop a model of the descending slab detached from the crust. The initial configuration of the slab and the crust were taken from the previous model.

Meissner and Mooney (1998) estimated the depth to potential decoupling zones between the descending lithospheric slab and crust by calculating lithospheric viscosity-depth curves based on reasonable geotherms and models of lithospheric composition. They found that zones of reduced viscosity are located within the lower crust and several tens of kilometres below the Moho. In this model we replace the lower crustal material brought to depths of 60 to 80 km due to slab pull by the mantle material. With this assumption, we introduce a break between the descending slab and crust. Instead of modelling the process of slab break-off itself, we concentrate on study of the stress evolution after slab detachment.

Figure 8 presents the model evolution of the detached slab for the next 8.5 Ma. Maximum shear stresses are still sufficiently high (~50 MPa) in the upper portion of the slab in 0.5 Ma after slab detachment (Fig. 8a, left panel). Moreover, the stress increases at depths about 60-80 km because of the replacement of less viscous lower crustal material by more viscous mantle material. The slab continues to pull the detached crust downwards, while it continues to sink to depths of about 500 km (Fig. 8b). Necking of the slab develops in its upper portion (at depths of 150 to 400 km), and around this narrow area the shear stresses are reduced. After about 8 Ma the slab reaches the lower boundary of the model which corresponds to the boundary between the upper and lower mantle (Fig. 8c). Maximum shear stresses in the slab drops to its lowest level (~10 MPa), and the slab can no longer control the dynamics of the overlying crust and uppermost mantle.

The mantle flow induced by the descent of the detached slab is presented in Fig. 8 (right panel). In 2 Ma after the slab detachment the flow is divided into two cells. The shallow cell above the slab involves the crust and uppermost mantle material in the circulation. The flow in the cell (with the rate of about 1 cm yr⁻¹) is associated with the isostatic rebound of the subducted crust. The deeper cell in the mantle is induced by the sinking slab, and its flow rate is about 5 cm yr⁻¹.

Fig. 7b shows that the Carpathians subside even after slab detachment (curve 5), although the subsidence slows down. In the model the rise of the Carpathians began in 2 Ma after the slab detachment (curve 6), but the upward movements in the crust and uppermost mantle started earlier (before the slab detachment, see

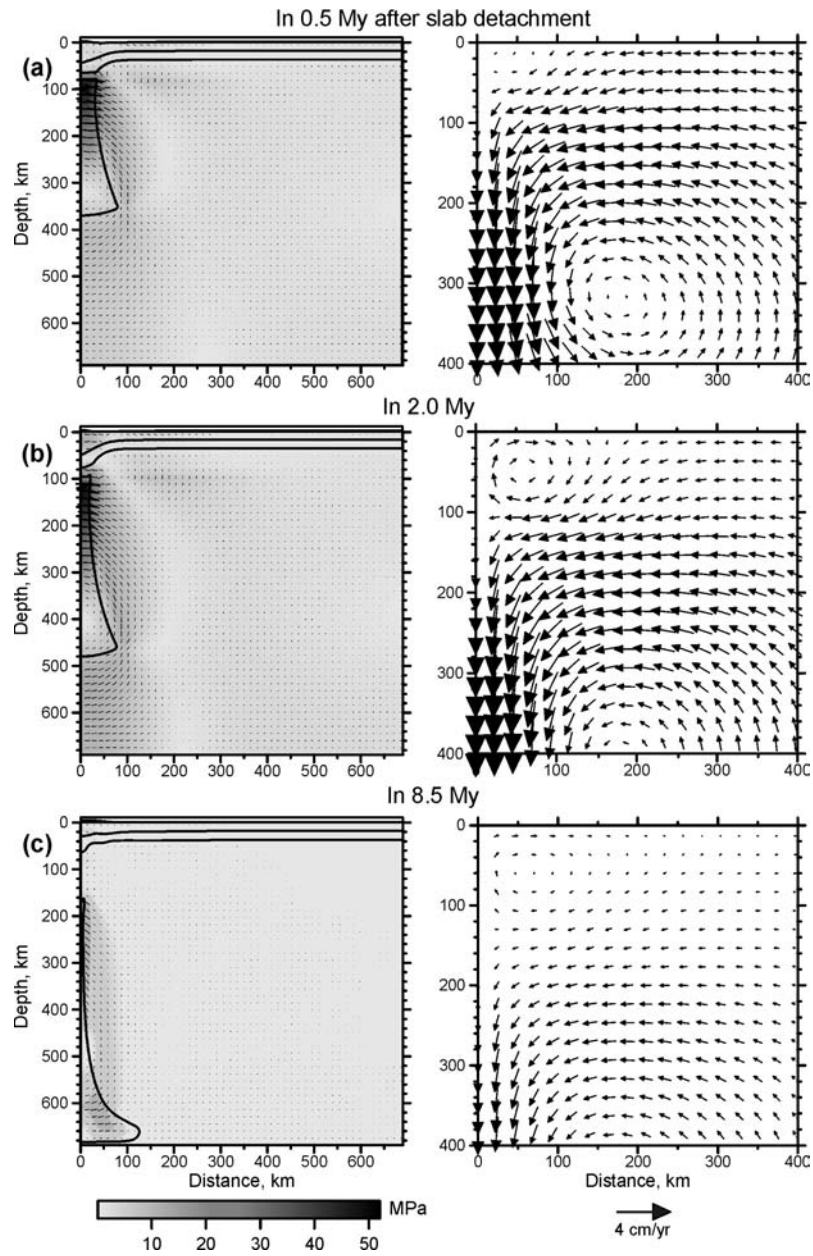


Fig. 8. Maximum tectonic shear stresses and axes of compression (left panel) and flow field (right panel) for the model evolution of the Vrancea slab (detached from the crust) descending in the mantle at successive times indicated (a)-(c).

Fig. 6c). The temporal shift between the surface uplift and upward movements in the crust can be attributed to a balance between forces, which pull the mountains down, and forces that push the crust upward due to isostasy.

Recent GPS studies on vertical movements in the Vrancea region revealed a relative uplift of the crust (Dinter et al. 2001). If the model prediction on the onset of the surface uplift is correct, it should be expected that the Vrancea slab is already detached from the crust.

Discussion and conclusions

There are essential distinctions between seismicity patterns of active subduction zones and those observed in continental collision zones. The subduction zone surrounding the Pacific ocean is an extended structure several thousands of km in length and a few hundreds of km in width. Earthquakes with focal depths up to 60 km dominate these regions. These events are associated with subducting lithospheric slabs of mostly shallow subduction angles, and their hypocentres are located at or near upper surfaces of the slabs. In contrast to the concentration of epicentres along this subduction zone, the seismicity of the continental collision zones (e.g. Alpine-Himalayan orogenic belt) is diffuse, reflecting the greater width of the deformation pattern of this type of plate boundary.

Intermediate-depth seismicity in the SE-Carpathians (Vrancea region) is concentrated near and along the south-eastern margin of the high-velocity body (Fig. 2). The margin is considered to be a lower surface of the slab during its active subduction. The location of earthquakes is obviously not compatible with Wadati-Benioff zones of subducting lithosphere where earthquakes are concentrated near the upper side of the slab.

Using an analytical model for corner flow, we have showed here that the pattern of tectonic stress, induced by a descending slab in active subduction zones, differs from that in passive subduction zones. Maximum shear stress migrates from the upper surface of the descending slab to its lower surface due to changes in dynamics of the descending slab (from active subduction to sinking due to gravity only). Hence we conclude that the seismicity pattern of the final stage of a descending lithospheric plate differs completely from the pattern familiar from Wadati-Benioff zones.

Intermediate-depth events observed in several places in the world (the Mediterranean region, Carpathians, Caucasus, Zagros, Pamir-Hindu Kush, and Assam; Ismail-Zadeh et al. 2000) are associated with plate collisions. High-resolution seismic tomography in the regions of intermediate-depth seismicity are crucial to answer the question: whether the seismic events in these regions are generally located at the lower surface of descending slabs or whether this is a unique feature of the Vrancea seismicity.

The finite-element thermomechanical model of a descending slab allows us to explain the seismic activity in Vrancea on the basis of analysis of shear stress: the axes of compression are close to the horizontal as it is observed; and the maximum

tectonic shear stress is found to be at depth of about 80 km to 180 km. The area of high maximum shear stress, predicted by the model, correlates with the region of Vrancea intermediate-depth events. The region of low seismicity at depths of 50 to 70 km is associated with a low viscosity zone in the model. An origin of the low viscosity zone might be due to either high temperatures at the relevant depths (Demetrescu and Andreescu 1994) or the lower crustal rocks brought down to the uppermost mantle depths during the slab descent.

An uplift of the crust begins before the initiation of slab detachment. The fate of the Vrancea slab is to be fully delaminated from the crust. The regional tectonic stresses are greatly reduced after following about 6 Ma slab detachment. The uplift and extension in the region predicted by the model are in a good agreement with observations in regions of slab detachment (e.g. Central Apennines, Wortel and Spakman 2000). The results of our analytical and numerical models together with seismic and geodetic observations allow interpreting the present-day dynamics of the Vrancea lithosphere as an ongoing process of detachment of the oceanic lithosphere from the overlying crust.

Acknowledgements. We are very grateful to Karl Fuchs who invited us to present the paper at the Symposium “Challenges for Earth Sciences in the 21st Century”. We thank W. Jacoby and J. Ritter for their constructive reviews of the manuscript. We are thankful to B. Sperner, F. Hauser, and M. Martin for useful discussions. Also we thank A. Wüstefeld for drawing of Fig. 2. This publication was supported by the Alexander von Humboldt Foundation and the Heidelberg Academy of Sciences and carried out under the auspices of the Collaborative Research Centre “Strong Earthquakes” (SFB 461).

References

- Batchelor GK (1967) An introduction to fluid dynamics. Cambridge University Press, New York
- Bijwaard H, Spakman W (2000) Non-linear global P-wave tomography by iterated linearized inversion. *Geophys J Int* 141: 71-82
- Demetrescu C, Andreescu M (1994) On the thermal regime of some tectonic units in a continental collision environment in Romania. *Tectonophysics* 230: 265-276
- Dinter G, Nutto M, Schmitt G, Schmidt U, Ghitau D, Marcu C (2001) Three-dimensional deformation analysis with respect to plate kinematics in Romania. *Reports on Geodesy*, 2: 1-21
- Forte AM, Mitrovica JX (2001) Deep-mantle high-viscosity flow and thermochemical structures inferred from seismic and geodynamic data. *Nature* 410: 1049-1056
- Fuchs K, Bonjer K, Bock G, Cornea I, Radu C, Enescu D, Jianu D, Nourescu A, Merkle G, Moldoveanu T, Tudorache G (1979) The Romanian earthquake of March 4, 1977. II. Aftershocks and migration of seismic activity. *Tectonophysics* 53: 225-247
- Gibracea R, Frisch W (1998) Slab in the wrong place: Lower lithospheric mantle delamination in the last stage of the Eastern Carpathian subduction retreat. *Geology* 26(7): 611-614

- Gutenberg B, Richter CF (1954) Seismicity of the Earth. Princeton University Press, Princeton, N.J., 2nd ed
- Hauser F, Raileanu V, Fielitz W, Bala A, Prodehl C, Polonic G, Schulze A (2001) VRANCEA99 – the crustal structure beneath the southeastern Carpathians and the Moesian Platform from a seismic refraction profile in Romania. *Tectonophysics* 340: 233-256
- Ismail-Zadeh AT, Keilis-Borok VI, Soloviev AA (1999) Numerical modelling of earthquake flows in the southeastern Carpathians (Vrancea): Effect of a sinking slab. *Phys Earth Planet Inter* 111: 267-274
- Ismail-Zadeh AT, Panza GF, Naimark BM (2000) Stress in the descending relic slab beneath the Vrancea region, Romania. *Pure Appl Geophys* 157: 111-130
- Linzer H-G (1996) Kinematics of retreating subduction along the Carpathian arc, Romania. *Geology* 24: 167-170
- Martin M, Achauer U, Kissling E, Mocanu V, Musacchio G, Radulian M, Wenzel F, Calixto working group (2001) First results from the tomographic experiment CALIXTO '99 in Romania. *Geophys Res Abst* 3: 84
- McKenzie DP (1969) Speculations on the consequences and causes of plate motions. *Geophys J R Astron Soc* 18: 1-32
- McKenzie DP (1972) Active tectonics of the Mediterranean region. *Geophys J R Astron Soc* 30: 109-185
- Meissner R, Mooney W (1998) Weakness of the lower continental crust: a condition for delamination, uplift, and escape. *Tectonophysics* 296: 47-60
- Naimark BM, Ismail-Zadeh AT, Jacoby WR (1998) Numerical approach to problems of gravitational instability of geostructures with advected material boundaries. *Geophys J Int* 134: 473-483
- Oncescu MC (1984) Deep structure of the Vrancea region, Romania, inferred from simultaneous inversion for hypocentres and 3-D velocity structure. *Ann Geophys* 2: 23-28
- Oncescu MC, Bonjer KP (1997) A note on the depth recurrence and strain release of large Vrancea earthquakes. *Tectonophysics* 272: 291-302
- Oncescu MC, Trifu CI (1987) Depth variation of moment tensor principal axes in Vrancea (Romania) seismic region. *Ann Geophys* 5: 149-154
- Sperner B, Lorenz F, Bonjer K, Hettel S, Müller B, Wenzel F (2001) Slab break-off – abrupt cut or gradual detachment? New insights from the Vrancea region (SE Carpathians, Romania). *Terra Nova* 13: 172-179
- Stevenson DJ, Turner JS (1977) Angle of subduction. *Nature* 270: 334-336
- Tovish A, Schubert G, Luyedyk BP (1978) Mantle flow pressure and the angle of subduction: non-Newtonian corner flow. *J Geophys Res* 83: 5892-5898
- Turcotte DL, Schubert G (2002) *Geodynamics*. Cambridge University Press, Cambridge, 2nd ed
- Wenzel F, Achauer U, Enescu D *et al.* (1998a) Detailed look at final stage of plate break-off is target of study in Romania. *EOS Transactions AGU* 79: 589-594
- Wenzel F, Lorenz FP, Sperner B, Oncescu MC (1998b) Seismotectonics of the Romanian Vrancea area. In: Wenzel F, Lungu D, Novak O (eds) *Vrancea Earthquakes: Tectonics, Hazard and Risk Mitigation*. Kluwer, Dordrecht, pp 15-25
- Wortel MJR, Spakman W (2000) Subduction and slab detachment in the Mediterranean-Carpathian region. *Science* 290: 1910-1917
- Zhao D. (2001) Seismological structure of subduction zones and its implications for arc magmatism and dynamics. *Phys Earth Planet Inter* 127: 197-214

**THREE-DIMENSIONAL NUMERICAL MODELING OF CONTEMPORARY
MANTLE FLOW AND TECTONIC STRESS BENEATH
THE EARTHQUAKE-PRONE SOUTHEASTERN CARPATHIANS**

Alik Ismail-Zadeh (1,2,3)*, Birgit Mueller (1), and Gerald Schubert (3)

- (1) Geophysical Institute, University of Karlsruhe, Hertzstr. 16, Karlsruhe 76187, Germany
- (2) International Institute of Earthquake Prediction Theory and Mathematical Geophysics, Russian Academy of Sciences, Warshavskoye shosse 79-2, Moscow 113556, Russia
- (3) Department of Earth & Space Sciences, UCLA, 3806 Geology Building, 595 Charles Young Drive East, Los Angeles, CA 90095-1567, USA

* Corresponding author:

Tel: +49-721-6084621

Fax: +49-721- 71173

E-mail: Alik.Ismail-Zadeh@gpi.uni-karlsruhe.de

Submitted to *Physic of the Earth and Planetary Interiors*

Abstract

The principal purpose of the study is to understand the interplay between intermediate-depth large earthquakes in the SE-Carpathians (Vrancea) and tectonic stress induced by a high-velocity body (lithospheric slab) descending into the mantle beneath the region. To analyze processes of stress generation and localization in and around the descending slab, we develop a 3D numerical model of contemporary mantle flow and stress beneath the Vrancea region. The input data of the model consist of (i) temperatures derived from seismic P-wave velocity anomalies and surface heat flow, (ii) crustal and uppermost mantle densities converted from P-wave velocities which were obtained from seismic refraction studies, (iii) geometry of the Vrancea crust and slab from tomography and refraction seismic data, and (iv) the estimated strain rate in the slab (as a result of earthquakes) to constrain the model viscosity. We find that major crustal uplifts predicted by the model coincide with the East Carpathian orogen and surround the Transylvanian basin and that predicted areas of subsidence are associated with the Moesian and East European platforms. We show a correlation between the location of intermediate-depth earthquakes and the predicted localization of maximum shear stress. Modeled tectonic stresses predict large horizontal compression at depths of about 70 to 220 km beneath the Vrancea region, which coincides with the stress regime defined from fault-plane solutions for the intermediate-depth earthquakes. This implies that buoyancy-driven descent of the lithospheric slab beneath the Vrancea region is directly linked to intermediate-depth seismicity.

Key words: descending slab, viscous stress, mantle flow, numerical modeling, Vrancea seismicity.

1. Introduction: Seismicity and geodynamics of the SE-Carpathians

Repeated large intermediate-depth earthquakes of the southeastern (SE) Carpathians (Vrancea region) cause destruction in Bucharest (Romania) and shake central and eastern European cities several hundred kilometers away from the hypocenters of the events. The earthquake-prone Vrancea region is situated at the bend of the SE-Carpathians and is bounded to the north and north-east by the Eastern European platform (EEP), to the

east by the Scythian platform (SP), to the south and south-west by the Moesian platform (MP), and to the north-west by the Transylvanian basin (TB). The epicenters of the mantle earthquakes in the Vrancea region are concentrated within a very small area (Fig. 1). The projection of the foci on a NW-SE vertical plane across the bend of the Eastern Carpathians (section AB in Fig. 1) shows a seismogenic volume about 110 km long, about 70 km × 30 km wide, and extending to a depth of about 180 km. Beyond this depth the seismicity ends suddenly: one seismic event at 220 km depth represents an exception (Oncescu and Bonjer, 1997). According to the historical catalogue of Vrancea events (Radu, 1979; 1991), large intermediate-depth shocks with magnitudes $M_W > 6.5$ occur three to five times per century. In the XXth century, large events at depths of 70 to 180 km occurred in 1940 (moment magnitude $M_W = 7.7$, $d = 160$ km deep), in 1977 ($M_W = 7.5$, $d = 100$ km), in 1986 ($M_W = 7.2$, $d = 140$ km), and in 1990 ($M_W = 6.9$, $d = 80$ km) (e.g., Oncescu and Bonjer, 1997).

The 1940 earthquake gave rise to the development of a number of geodynamic models for this region. Gutenberg and Richter (1954) drew attention to the Vrancea region as a place of remarkable intermediate-depth seismicity. Later McKenzie (1972) suggested this seismicity to be associated with a relic slab sinking in the mantle that is now overlain by continental crust. The 1977 disastrous earthquake and later the 1986 and 1990 earthquakes led to renewed discussion of the nature of the earthquakes. A seismic gap at depths of 40-70 km beneath Vrancea led to the assumption that the lithospheric slab had already been detached from the continental crust (Fuchs et al., 1979). Oncescu (1984) proposed that the intermediate-depth events are generated in a zone that separates the sinking slab from the neighboring immobile part of the lithosphere rather than in the sinking slab itself. Linzer (1996) explained the nearly vertical position of the Vrancea slab as the final rollback stage of a small fragment of oceanic lithosphere, and Gîrbacea and Frisch (1998) assumed that the break-off, affecting only the crustal portion of the slab, was followed by horizontal delamination of its lower portion. Most recently Sperner et al. (2001) suggested a model of Miocene subduction of oceanic lithosphere beneath the Carpathian arc and subsequent soft continental collision, which transported cold and dense lithospheric material into the mantle.

Subduction in the SE-Carpathians ceased about 10 Ma ago (Jiricek, 1979; Csontos et al., 1992). Subsequently, the initial subduction zone began to steepen to its present-day nearly vertical orientation. At present the cold slab (hence denser than the surrounding

mantle) beneath the Vrancea region sinks due to gravity. The hydrostatic buoyancy forces promote the sinking of the slab, but viscous and frictional forces resist the descent. The combination of these forces produces shear stresses at intermediate depths, which are high enough to cause earthquakes. This was shown in two-dimensional numerical models of mantle flow and tectonic stress by Ismail-Zadeh et al. (2000). These authors recognized that the depth distribution of the annual average seismic energy released in earthquakes has a shape similar to that of the depth distribution of the modeled stress magnitude in the slab.

To evaluate the role of slab detachment in stress evolution, Ismail-Zadeh et al. (2003a) developed two-dimensional thermo-mechanical finite-element models of the post-Miocene subduction of the Vrancea slab subject to gravity forces alone. The models predicted lateral compression in the slab that were in agreement with those inferred from the stress axes of earthquakes. It was found that the maximum stress occurs in the depth range of 80 km to 200 km and the minimum stress falls into the depth range of 40 km to 80 km, which corresponds to the seismic gap. It was also shown that high tectonic stress (to lead to seismic activity) is preserved in the slab for a few million years even after the detachment. The two-dimensional numerical studies revealed principal features of mantle flow and tectonic stresses induced by a simple model of the descending slab, but they could not show a correlation between the descending high-velocity body, tectonic stress, and the locations of the Vrancea intermediate-depth earthquakes in any detail.

The principal purposes of this research are to understand (i) how the uppermost mantle structure beneath the SE-Carpathians relates to the intermediate-depth seismicity in the Vrancea region and (ii) how these seismic events correlate with the tectonic stresses induced by the descending lithospheric slab. Hence, we developed a 3D numerical finite-element model of the instantaneous viscous flow and tectonic stress in the region where input model parameters (geometry, temperature, density, viscosity) are based on the results of regional seismic tomography, seismic refraction, and the modeling of density, gravity, and temperature. We summarize the results of the recent seismic tomographic study conducted in the SE-Carpathians in section 2.1, the results of two international projects on seismic refraction studies in the region in sect. 2.2, the results of the density modeling in the SE-Carpathians and of the regional gravity modeling in sect. 3. We discuss possibilities for deriving temperature of the mantle (sect. 4.1) and crust (sect. 4.2) from the seismic and heat flow data and present results of the temperature modeling

beneath the SE-Carpathians. The model of mantle and crustal flow and of tectonic stress in the region is described in sect. 5.1, the predicted flow in sect. 5.2, and tectonic stress in sect. 5.3. Then we discuss the model results, the limitations and uncertainties of the study, and conclude the research.

2. Seismic studies of the SE-Carpathians

2.1. Seismic tomography

In 1999 the international tomographic experiment CALIXTO with 143 seismic stations was conducted in the southeastern Romania (Martin et al., 2001). During the field experiment 160 local events with magnitude $M_l \geq 2.0$ and 450 teleseismic events with magnitude $M_b \geq 5.0$ were recorded. The distance between stations ranged from 15-20 km (the Vrancea region) to 25-30 km (outer margins of the network), covering a region of about 350 km in diameter. First results were achieved through an inversion of the teleseismic data with the ACH method (Aki et al., 1977; Evans and Achauer, 1993). Crustal complexity causes a smearing of these results for the upper 60 km. This can be overcome if travel times are calculated through a realistic regional crustal model (Martin et al., 2003). Varying crustal thickness and young deep basins, like the Focsani foredeep basin with its 9 km of Neogene to Quaternary sediments, have to be considered. In such a more sophisticated analysis, the boundaries of the anomalies might shift by at most 20 km. Nevertheless, the results for the deeper parts are reliable enough for the present study to fix the general shape of the velocity anomalies.

Data inversion reveals a high-velocity body with maximum P-wave velocity perturbations of +3.5% in comparison with the background model (see Fig. 2). This high-velocity body is interpreted as the descending lithospheric slab. It reaches a depth of at least 350 km (this is a maximum depth of high resolution tomography), which is in good agreement with results of previous seismic tomography studies (e.g., Wortel and Spakman, 2000). The tomography images reveal features not visible in previous studies by Oncescu (1984), Wenzel et al. (1999), and Bijwaard and Spakman (2000), and allow determination of the geometry of the descending slab and its spatial relation to the earthquake hypocenters.

Because the upper limit of the high-velocity body cannot be presently defined from the seismic tomography images, we use in our analysis the results of the refraction seismic investigations.

2.2. Seismic refraction study

Two active-source seismic experiments (in 1999 and 2001) were carried out in the SE-Carpathians to study the crustal and uppermost mantle structure and physical properties beneath the Vrancea region (Hauser et al., 2001; 2002). The 300 km long VRANCEA99 and the 400 km long VRANCEA2001 seismic refraction profiles crossed the Vrancea epicentral area in NNE–SSW and ESE–WNW directions, respectively (Fig. 1). Using forward and inverse ray trace modeling Hauser et al. (2001, 2002) distinguished a multi-layered crust with lateral velocity variations in the sedimentary cover and minor changes in the crystalline crust. They showed that the sedimentary succession comprises two to four seismic layers of variable thickness with velocities ranging from 2.0 to 5.8 km s⁻¹. The upper limit of the seismic basement coincides with a velocity of 5.9 km s⁻¹, velocities in the upper crystalline crust are 5.9–6.2 km s⁻¹. An intra-crustal discontinuity apparent at depths between 18 to 31 km divides the crust into an upper and a lower layer.

The Moho discontinuity is predicted at a depth of about 40 km near the intersection of these profiles. Hauser et al. (2002) reported that the Moho shows no crustal roots under the Carpathians. Velocities are 6.7–7.0 km s⁻¹ within the lower crust and about 7.9 km s⁻¹ just below the Moho. Hauser et al. (2001) found a low-velocity zone (7.6 km s⁻¹) within the uppermost part of the mantle (at depths of 45 to 55 km) and the velocity beneath this zone is at least 8.5 km s⁻¹. This low velocity zone coincides with the seismic gap at depths of 40–70 km (Oncescu, 1984).

3. Density and gravity modeling

Based on the seismic velocity models obtained from the refraction experiments and seismic tomography, we derived a 3D density model using the empiric velocity (v_p) to density (ρ) relationships derived by Krasovsky (1989):

$$\rho = 0.7212 + 0.3209v_p .$$

Krasovsky (1989) summarized and processed experimental data on this relationship at high pressures for more than 2000 samples of various crystalline rocks worldwide taking into consideration the rock composition and metamorphic grade.

On the basis of the derived density models, Hackney et al. (2002) developed a 3D gravity model of the SE-Carpathians employing the IGMAS software for gravity modeling (Schmidt and Götze, 1998). It was shown that the gravity effect predicted for the Vrancea slab is about +20 mGal. When the slab gravity effect is removed from the observed Bouguer anomalies (Ioane and Atanasiu, 1998), the signature associated with the Carpathian foredeep (most negative Bouguer anomalies) is modified to more negative values. Hackney et al. (2002) suggested that this modified anomaly pattern might better reflect the geometry of the foredeep basin.

4. Temperature modeling

This section of the paper is based on the results of temperature modeling beneath the SE-Carpathians described in more detail by Ismail-Zadeh et al. (2003b). We present the results of temperature modeling here too to clarify our subsequent description of flow and stress modeling.

Temperature is a key physical parameter controlling the density, viscosity and rheology of the Earth's material and hence crustal and mantle dynamics. Information on temperature inside the Earth's shallow crust comes from direct measurements of temperature in boreholes. There are however no direct measurements of deep crustal and mantle temperatures, and therefore the temperatures can be estimated indirectly from either seismic wave anomalies, geochemical analysis or through the extrapolation of surface heat flow observations.

4.1. Mantle temperatures from P-wave tomography

Seismic waves allow for 3D imaging of seismic velocities of the Earth's interior. The seismic velocity anomalies in the upper mantle can be attributed to variations in temperature (Forte et al., 1994, 1995), although several factors other than temperature can also exert an influence on seismic velocity: composition (Griffin et al., 1998), anelasticity (Karato, 1993), anisotropy and presence of melt or water (Karato, 2003). Uppermost

mantle composition has a complex effect on seismic velocity, while the effect is relatively small compared to the effect of temperature (Jordan, 1979; Sobolev et al., 1996, Goes et al., 2000). During peridotite melting, garnet and clinopyroxene (fastest and slowest of four major minerals which compose the upper mantle) concentrate in the melt (Niu, 1997), and therefore the change in composition of peridotite, as it melts and the melt is extracted, does not appear to significantly affect seismic velocities (Jordan, 1979). Meanwhile the presence of melt may have an effect on seismic velocities.

Seismic wave velocities are affected by melting depending on the melt fraction and geometry. Takei (2000) and Hammond and Humphreys (2000a,b) showed that for a reasonable range of geometries, partial melting has an important effect on seismic wave velocities when the melt fraction exceeds ~1%. The melt fraction for a given material is controlled by the degree of partial melting and the efficiency of melt transport, and the degree of partial melting is determined by temperature and water content. Interpretation of seismic anisotropy is not always unique, because of a trade-off between mantle flow geometry and physical mechanisms of anisotropic structure formation (e.g., Smith et al., 2001). Therefore, in the forward modeling of synthetic P-wave seismic velocity anomalies beneath the SE-Carpathians the effects of anharmonicity (composition), anelasticity and partial melting on seismic velocities were considered.

The seismic tomographic model of the SE-Carpathians we used to derive temperature consists of nine layers of different thickness, which are each subdivided into rectangular blocks (Martin et al., 2001). To restrict numerical errors in the subsequent analysis of flow and tectonic stress we smooth the velocity anomaly data using spline interpolations between the blocks and the layers.

The anharmonic (frequency independent and non-attenuating) part of the synthetic velocities was calculated on the basis of published data on laboratory measurements of density and elastic parameters of the main rock-forming minerals (e.g., Bass, 1995) at various thermodynamic conditions for the composition of the crust and mantle (57.9% Ol, 16.3% CPx, 13.5% Opx, and 12.3% Gt; Green and Falloon, 1998) and the slab (69% Ol, 10% CPx, 19% Opx, and 2% Gt; Agee, 1993). The methodology described by Goes et al. (2000) was used to derive the anharmonic part of the synthetic velocities. To evaluate the effects of anelasticity (attenuation and frequency dependence) and melting, a methodology similar to Sobolev et al. (1996) was employed. Once the synthetic velocities are calculated for a first-guess temperature, an iteration process is used to find the 'true' temperature,

minimizing the difference between the synthetic and ‘observed’ (in seismic tomography experiments) velocities. During the conversion of seismic velocity to temperature, the reference (background) temperature should be introduced. The laterally averaged temperature in the crust and mantle modeled by Demetrescu and Andreescu (1994) was chosen as the background temperature for the inversion (Fig. 3).

The mantle temperatures at depths of 90, 120, 150 and 200 km are presented in Fig. 4. The pattern of resulting mantle temperature anomalies (predicted temperature minus background temperature) is similar to the pattern of observed P-wave velocity anomalies (Martin et al., 2001). Lowest temperatures are associated with the high-velocity body beneath the Vrancea region, and high temperatures are predicted under the Transylvanian depression and the regions of Neogene magmatism in the eastern Carpathians.

4.2. Crustal and uppermost mantle temperatures from heat flow

Smearing of the results of seismic tomography for the upper 60 km does not allow for correct estimations of the temperature in the crust and uppermost mantle. The temperature in the shallow levels of the Romanian region was modeled from measured surface heat flux corrected for paleoclimate changes in the last 70 Ka ($+8 \text{ mW m}^{-2}$) and for the effects of sedimentation on temperatures in the crust in the Focsani and Transylvanian depressions (Demetrescu et al., 2001). A 1-D temperature distribution with depth was calculated starting from the measured surface heat flux, assuming steady-state conduction of heat through the lithosphere and adopting a certain model of thermal parameters (thermal conductivity and heat production) characterizing the various subdivisions of the crust and upper mantle. The analytical solution to the steady-state conduction equation of the heat transfer in a multi-layered medium was used (Demetrescu and Andreescu, 1994).

Figure 5 presents the temperatures at depths of 20 and 50 km. The high temperatures beneath the Neogene volcanic area (25-26°E, 46-47°N) are associated with the high surface heat flux ($>80 \text{ mW m}^{-2}$). Depending on the crustal model adopted for the volcanic activity (in the presence or absence of magmatic chambers with high temperature in the crust), temperatures might differ in the depth range of 20 to 50 km. The presented values of temperature come from a model without magma chambers in the crust (C. Demetrescu, pers. com.)

5. Mantle flow and stress

5.1. Model description

To study the effects of the slab on tectonic stress in the region, we develop a 3D numerical model of the descending Vrancea slab based on realistic (in sense of the seismic tomographic image) slab geometry. We consider the model interface between the Vrancea slab and the surrounding mantle to coincide with the surface of 2%-positive anomaly of P-wave seismic velocity obtained in the regional seismic tomography study (see Fig. 2). The interface between the crust and mantle in the model is a 3D extrapolation of the Moho discontinuity found in the seismic refraction studies (Hauser et al., 2001, 2002). The model structure comprises the crust, slab, and uppermost mantle (down to 350 km). With respect to our 2D numerical analysis of tectonic stress (Ismail-Zadeh et al., 2000, 2003a), which assumed a simplified geometry and physical parameters, we add now some complexities such as the realistic geometry, temperature distribution based on seismic and heat flow data, temperature-dependent density, and temperature- and pressure-dependent viscosity. These complexities permit a more detailed comparison between model predictions and observations.

In the model domain $\Omega: \{0 \leq x_1 \leq l_1, 0 \leq x_2 \leq l_2, 0 \leq x_3 \leq l_3\}$ (where $\mathbf{x} = (x_1, x_2, x_3)$ are the Cartesian coordinates), we consider an inhomogeneous viscous mantle flow in the presence of gravity. The flow is described by the momentum (Stokes) equation

$$-\nabla P + \text{div}\{\mu(T, P)e_{ij}\} + \rho(T)g = 0, \quad (1)$$

the incompressibility condition

$$\text{div } \mathbf{u} = 0, \quad (2)$$

the equation of state for density

$$\rho(T) = \rho_*(x_3)[1 - \alpha(T - T_*)], \quad (3)$$

and the temperature-and-pressure dependent viscosity

$$\mu(T, P) = \mu_*(\mathbf{x}) \exp\left(\frac{E + PV}{RT} - \frac{E + P_0V}{RT_*}\right), \quad (4)$$

where P is pressure, μ is viscosity, ρ is density, T is temperature, $\mathbf{u} = (u_1, u_2, u_3)$ is the flow velocity, $e_{ij} = 0.5 (\partial u_i / \partial x_j + \partial u_j / \partial x_i)$ is the strain-rate tensor, g is the acceleration due to gravity, α is the coefficient of thermal expansion, P_0 is pressure at the surface, E is the activation energy, V is the activation volume, R is the universal gas constant, and $\rho_*(x_3)$, $\mu_*(\mathbf{x})$, and $T_*(x_3)$ are the background density, viscosity, and temperature, respectively.

We consider laterally averaged densities in the crust and subcrustal mantle derived from the P-wave velocities (see Table 1 and Fig. 3) as the background density $\rho_*(x_3)$ for the 50-km upper layer of the model. The background density for the modeled mantle is based on the PREM model (Dziewonski and Anderson, 1981). The background temperature is derived from results of geothermal modeling of Vrancea lithosphere (Demetrescu and Andreescu, 1994) (Fig. 3).

Viscosity is an important physical parameter in stress modeling, because it influences the stress state and results in strengthening or weakening of Earth's material. Being the least-known physical parameter of the model, the viscosity of the Vrancea slab can, however, be constrained by observations of the regional strain rates. Intermediate-depth earthquakes in the Vrancea region provide an indirect measure of the rate of strain release within the seismogenic body (8×10^{18} N m yr⁻¹, Wenzel et al., 1999; Ismail-Zadeh et al., 2000). Therefore, the strain rate (ratio between stress and viscosity), as a result of the Vrancea earthquakes, is estimated to be 7.5×10^{-15} s⁻¹ (Wenzel et al., 1999; the estimation is based on Kostrov's (1974) formula). This strain rate was used as a constraint on the viscosity of the model slab in our test computations of the flow (and strain rate) for various viscosity ratios between slab and mantle. Based on these tests we adopted the background viscosity $\mu_*(\mathbf{x})$ to be 10^{22} Pa s for the Vrancea slab, 10^{23} Pa s for the crust, and 10^{20} Pa s for the mantle. The model parameters are summarized in Table 2.

We consider free-slip conditions at the upper and lower boundaries of the model domain and symmetry conditions at the side (vertical) boundaries. To avoid an effect of the lateral boundary conditions on the numerical results, we extended the modeled domain in horizontal directions by a factor of two. The effect of the surface loading due to the Carpathian Mountains is not considered, because this loading would have insignificant influence on the stress in the slab (as was shown in two-dimensional models of the

Vrancea slab evolution; Ismail-Zadeh et al., 2003a). According to the geodynamic models for the region (e.g., Sperner et al., 2001), the Vrancea slab, being at its late evolutionary stage, sinks into the mantle solely under the influence of gravity. Hence, neither horizontal or vertical velocities are superimposed on the model domain, and flow and induced tectonic stresses are considered to be due to buoyancy forces alone.

The numerical solution to the problem is based on the introduction of a two-component vector velocity potential (replacing the three components of vector velocity in Eqs. 1 and 2) and on the application of the Eulerian finite-element method with a tricubic-spline basis for computing the vector potential (Ismail-Zadeh et al, 2001). The tensor of tectonic stress σ_{ij} is then computed using the relationship $\sigma_{ij} = \mu(T, P) e_{ij}$.

The numerical models, with a spatial resolution of 10 km x 10 km x 5 km, were run on an IBM SP2 parallel computer. The accuracy of the solutions has been verified by several tests, including numerical grid changes and total mass changes (Ismail-Zadeh et al, 2001) and comparison with the simple analytical solution to the problem (Trushkov, 2002).

5.2. Predicted crustal and mantle flow

Figure 6 presents the 3D pattern of the flow predicted by the model. The main feature is that the gravitational sinking of the slab beneath the Vrancea region induces downwelling (blue cones) and associated upwelling (orange cones) in the mantle. In fact, the 3D flow is rather complicated at the depths associated with the intermediate-depth seismicity: the toroidal (in horizontal planes) flow at depths between about 100 to 200 km is coexistent with the poloidal (in vertical planes) flow. It should be noted that the horizontal flow at the bottom of the model is related to the prescribed boundary conditions and is an artifact. This shortcoming is associated with the fact that the slab can be seen in seismic tomographic images to depths of 350 km, and we have no information on either the presence or absence of the high-velocity anomaly deeper in the mantle. Hence, to avoid the ambiguity with the length of the slab in the modeling and keeping in mind that our aim is to evaluate flow and stress in the region at depths between 70 to 220 km where large earthquakes occur, we adopted the depth of the model domain to be 350 km.

The modeled vertical movements in the crust are shown in Fig. 7 (horizontal slice at depth of 15 km). The areas of major uplift in the model coincide with the East

Carpathian and Dobrogea orogens and surround the Transylvanian basin. These model findings are corroborated by the results from fission track analysis in the eastern Carpathian region and Transylvanian basin that demonstrate uplift of several hundred meters since at least Pliocene times (Sanders et al., 1999; 2002). The areas of modeled subsidence correlate with the Moesian and East European platforms. The numerical results on vertical crustal movements in the SE-Carpathians agree with the results of geomorphological, geodetical and geological analysis of recent crustal movements in the region (Radulescu et al., 1996; Zugravescu et al., 1998).

We want to emphasize that the pattern of vertical crustal movements should be considered in a qualitative way (while the results are quantitative) for the following reasons. First, knowledge of the physical properties (density, effective viscosity, temperature) of the crust in the SE-Carpathians is still poor, despite the existence of the seismic crustal models based on the two refraction profiles and results of regional geological and geothermal studies. Second, we do not know much about the rheology of the lower crust, which may influence the vertical movements of the upper crust (Andreescu and Demetrescu, 2001; Lenkey et al., 2002). Third, the reported GPS rates of vertical movements in the region (Dinter et al., 2001) were overestimated (G. Dinter, 2003, pers. com.). Ongoing GPS campaigns will probably provide better constraints on the vertical movements in the SE-Carpathian region in the near future. Fourth, the comparison of short-term GPS rates of surface movements with the predicted long-term movements due to mantle dynamics should be done very carefully in *seismically active* regions. The crustal deformations in such regions comprise post-seismic and tectonic deformations, which should be taken into consideration during a quantitative comparison.

5.3. Predicted tectonic stress

To examine whether the predicted areas of stress localization are consistent with the areas of the intermediate-depth seismicity in the region, we compare the predicted zones of maximum shear stress localization with the hypocenters of intermediate-depth earthquakes. The maximum shear stress (see Appendix 1 for the stress calculation) on the NW-SE cross-section through the Vrancea region is presented in Fig. 8. The stress is localized in a narrow zone that coincides with the projection of earthquake hypocenters onto the same cross-section. The calculated maximum shear stress is also shown in

horizontal planes at depths of 90, 120, 150, and 200 km in Fig. 9. The predicted maximum shear stress is associated with the descending Vrancea slab (cold lithospheric body), localized at depths of about 80 km to 180 km, diminishes to the depth of 220 km, and encompasses the area of major Vrancea intermediate-depth events.

The stress concentration in the Vrancea slab during a period between two large earthquakes could have some important implications for the location of a future rupture. Chinnery (1963) showed that shear stresses rise in an area much wider than just in the area of fault tips. The importance of the Chinnery's discovery was realized later, when lobes of off-fault aftershocks were seen to be associated with calculated increases in shear or Coulomb failure stress (Stein, 1999, and references therein).

Another result of the model is the maximum horizontal stress (see Appendix 1 for the stress calculation). Figure 10 illustrates the maximum horizontal stress at depths of 90, 120, 150, and 200 km. The horizontal compression is localized in the areas of large earthquakes. Using numerous fault-plane solutions for intermediate-depth events, Oncescu and Trifu (1987) showed that the axes of compressional stress are almost horizontal (see Fig. 2). The complex geometry of the zone of maximum compressional stress reflects the pattern of flow induced by the Vrancea slab sinking in the mantle under the influence of gravity.

Discussion

We have modeled tectonic stresses induced by the descending high-velocity body (interpreted as a relic lithospheric slab) beneath the SE-Carpathians (Vrancea earthquake-prone region) and shown that the seismic events at intermediate depths are associated with the zones of maximum shear stress localization. Horizontal compression at these depths agrees well with the stress determination based on the focal mechanisms of the intermediate-depth earthquakes. Small-scale discrepancies between the model predictions and regional observations can be attributed to the model limitations and uncertainties discussed below.

An interpretation of absolute values of lateral heterogeneities in seismic wave velocities has uncertainties regarding thermal anomaly or differences in chemical composition. Moreover, a refined model of P-wave seismic tomography that considers crustal structure can improve the current model at uppermost mantle depths. Another

source of uncertainty comes from the choice of mantle and slab compositions in the modeling of mantle temperature from the P-wave seismic velocities. Unfortunately, there are no data on the composition of the mantle beneath the SE-Carpathians, except a few petrological studies of igneous rocks from the Neogene eastern Carpathian volcanic zone (Nitoi et al., 2002, and references therein).

As direct temperature measurements are limited to depths of a few km from the surface, the information on the average temperature versus depth comes from geothermal conductivity modeling (Demetrescu and Andreescu, 1994). Additional information from geothermobarometry of xenoliths may better constrain the background temperature profiles (Sobolev et al., 1996).

Viscosity in the mantle beneath the Vrancea region might be influenced by the presence of water at 50 to 100 km depth. In the modeling, we used a temperature- and pressure-dependent viscosity for the mantle and did not take into account the dependence of viscosity on water. Mei et al. (2002) showed that, due to the combined effects of water and melt weakening, the mantle viscosity in subduction zones can vary by three orders of magnitude over the depth-range 60 to 120 km.

Despite the model limitations, we have demonstrated the causal relationship between tectonic stress and seismic activity in the region as a consequence of viscous flow induced by the Vrancea slab descending into the mantle under the influence of gravity. Moreover, we have showed that our parsimonious model (in terms of the numbers of tuning model parameters) can provide a sound interpretation of the observed seismic data.

In addition to viscous stress induced by the descending Vrancea slab, other processes might contribute to the stress generation. An increase of shear stress due to the descending slab is one of the possibilities analyzed here. Another process could be a plastic instability at high temperature, when runaway shear slip (failure) occurs at even relatively low shear stresses (Griggs and Baker, 1969). Faulting due to metamorphic phase transitions (Green and Burnley, 1989) or dehydration-induced embrittlement (Raleigh and Paterson, 1965; Hacker et al., 2003) may also play a role in the regional stress generation and release. However, estimations of the cumulative annual seismic moment observed and associated with the volume change due to the basalt-eclogite phase changes in the Vrancea slab show that a pure phase-transition model cannot solely explain the intermediate-depth earthquakes in the region (Ismail-Zadeh et al., 2000).

The question that remains is why earthquakes are located only in a part of the maximum shear stress zone (see Fig. 9). Ismail-Zadeh (2003) attempted to answer this question by making use of a simple analytical model for corner flow (Batchelor, 1967). He demonstrated that the pattern of tectonic stress, induced by a descending slab in subduction zones, differs from that in zones of collision. Maximum shear stress migrates from the upper surface of the descending slab to its lower surface due to changes in dynamics of the descending slab (from slab subduction due to applied lateral forces to slab retreat due to gravity forces). Moreover, as shown in the block-and-fault model of the Vrancea region (Ismail-Zadeh et al., 1999; Soloviev and Ismail-Zadeh, 2003), large earthquakes are likely to occur at the lower surface of the descending slab rather than at its upper surface.

Intermediate-depth earthquakes observed in several places in the world (Pamir-Hindu Kush, the Mediterranean region, Caucasus, Zagros, and Assam) are associated with plate collisions. However, due to the lack of tomography studies, the distribution of earthquake hypocenters with respect to the descending slab beneath these regions is not as well constrained as in the Vrancea region. High-resolution seismic tomography in the regions of intermediate-depth seismicity are crucial (i) to answer the question on *hypocenter locations with respect to the descending slab* and (ii) to clarify *the role of buoyancy forces in contemporary stress generation, its localization and association with seismic events*.

Conclusion

Based on data from seismic tomography, seismic refraction profiles, heat flow and on the knowledge of geodynamic evolution of the region, we have performed the quantitative analysis of contemporary slow mantle flow and tectonic stress beneath the SE-Carpathians. We have demonstrated a correlation between the location of intermediate-depth earthquakes and the predicted localizations of maximum shear stress and horizontal compression. Therefore, the buoyancy forces, which result from realistic temperature and density distributions in the crust and mantle, can govern the present-day deformation beneath the SE-Carpathians and explain the regional stress pattern and intermediate-depth seismicity. Refined seismic tomography results and geothermal modeling will improve the present tectonic stress model.

Acknowledgements. We are very grateful to M. Martin for providing the data on seismic tomography, M. Andreescu and C. Demetrescu for the regional crustal temperature models and fruitful discussions on the geothermal evolution of the region, to K. Bonjer, J. Dirkzwager, K. Fuchs, R. Hackney, F. Hauser, S. Karato, J. Ritter, B. Sperner, and F. Wenzel for useful discussions on the regional seismicity, geodynamics, gravity, and temperature modeling and critical comments on initial versions of the manuscript. We also thank A. Wüstefeld for assistance in digital data preparation and drawing several figures. This publication was supported by the Alexander von Humboldt Foundation (to A.T.I-Z) and the National Science Foundation (EAR 0105945).

Appendix 1. Calculation of principal stress, maximum shear stress, and maximum horizontal stress from the deviatoric stress tensor.

The principal stresses $\sigma_1 \geq \sigma_2 \geq \sigma_3$ are the roots of the cubic equation (e.g., Jaeger and Cook, 1984)

$$\sigma^3 - I_1\sigma^2 - I_2\sigma - I_3 = 0,$$

where I_k ($k=1,2,3$) are three invariants of the deviatoric (tectonic) stress tensor:

$$I_1 = \tau_{11} + \tau_{22} + \tau_{33},$$

$$I_2 = -(\tau_{11}\tau_{22} + \tau_{11}\tau_{33} + \tau_{22}\tau_{33}) + \tau_{12}^2 + \tau_{13}^2 + \tau_{23}^2,$$

$$I_3 = \tau_{11}\tau_{22}\tau_{33} + 2\tau_{12}\tau_{13}\tau_{23} - \tau_{11}\tau_{23}^2 - \tau_{22}\tau_{13}^2 - \tau_{33}\tau_{12}^2.$$

Using the Cardano's formula, we find an analytical expression of the principal stresses from the cubic equation:

$$\sigma_{1,2,3} = \left[-\frac{q}{2} + \left(\frac{q^2}{4} + \frac{p^3}{27} \right)^{1/2} \right]^{1/3} + \left[-\frac{q}{2} - \left(\frac{q^2}{4} + \frac{p^3}{27} \right)^{1/2} \right]^{1/3},$$

where

$$p = -\frac{1}{3}I_1^2 - I_2, \quad q = -\frac{2}{27}I_1^3 - \frac{1}{3}I_1I_2 - I_3.$$

The maximum shear stress τ_{\max} is calculated from the principal stresses:

$$\tau_{\max} = 0.5(\sigma_1 - \sigma_3)$$

The maximum horizontal stress S_H is calculated from the tensor of tectonic stress τ_{ij} as

$$S_H = \max(\theta_{13}, \theta_{23})$$

where

$$\theta_{13} = \tau_{23} \sin \alpha + \tau_{13} \cos \alpha, \quad \theta_{23} = \tau_{23} \cos \alpha - \tau_{13} \sin \alpha$$

and $\alpha = 0.5 \arctan \frac{2\tau_{12}}{\tau_{11} - \tau_{22}}$.

References

- Agee, C.B., 1993. Petrology of the mantle transition zone. *Ann. Rev. Earth Planet. Sci.*, 21: 19-41.
- Aki, K., Christofferson, A., and Husebye, E.S., 1977. Determination of the three dimensional seismic structure of the lithosphere. *J. Geophys. Res.*, 82: 277-296.
- Andreescu, M., and Demetrescu, C., 2001. Rheological implications of the thermal structure of the lithosphere in the convergence zone of the Eastern Carpathians. *J. Geodyn.*, 31: 373-391.
- Bass, J.D., 1995. Elasticity of minerals, glasses, and melts. In: T.J. Ahrens (Editor). *Mineral Physics and Crystallography, A Handbook of Physical Constants*. Am. Geophys. Union: 45-63.
- Batchelor, G.K., 1967. *An Introduction to Fluid Dynamics*. Cambridge University Press, Cambridge, 615 pp.
- Bijwaard, H., and Spakman, W., 2000. Non-linear global P-wave tomography by iterated linearized inversion. *Geophys. J. Int.*, 141: 71-82.
- Chinnery, M.A., 1963. The stress changes that accompany strike-slip faulting. *Bull. Seismol. Soc. Am.*, 53: 921-932.
- Csontos, L., Nagymarosy, A., Horvath, F., and Kovac, M., 1992. Tertiary evolution of the intra-Carpathian area; a model. *Tectonophysics*, 208: 221-241.
- Das, S., and Scholz, C. H., 1981. Off-fault aftershock clusters caused by shear stress increase? *Bull. Seismol. Soc. Am.*, 71: 1669-1675.
- Demetrescu, C., and Andreescu, M., 1994. On the thermal regime of some tectonic units in a continental collision environment in Romania. *Tectonophysics*, 230: 265-276.
- Demetrescu, C., Nielsen, S.B., Ene, M., Serban, D.Z., Polonic, G., Andreescu, M., Pop, A., and Balling, N., 2001. Lithosphere thermal structure and evolution of the Transylvanian Depression – insight from new geothermal measurements and modelling results. *Phys. Earth Planet. Int.*, 126: 249-267.

- Dinter, G., Nutto, M., Schmitt, G., Schmidt, U., Ghitau, D., and Marcu, C., 2001. Three dimensional deformation analysis with respect to plate kinematics in Romania. *Reports on Geodesy*, 2: 29-42.
- Dziewonski, A.M., and Anderson, D.L., 1981. Preliminary Reference Earth Model (PREM). *Phys. Earth Planet. Int.*, 25: 297-356.
- Evans, J.R., and Achauer, U., 1993. Teleseismic velocity tomography using the ACH-method: Theory and application to continental-scale studies. In: K.M. Iyer and K. Hirahara (Editors). *Seismic Tomography; Theory and Practice*. Chapman and Hall, London: 319-360.
- Forte, A.M., Woodward, R.L., and Dziewonski, A.M., 1994. Joint inversions of seismic and geodynamic data for models of three-dimensional mantle heterogeneity. *J. Geophys. Res.*, 99: 21,857-21,887.
- Forte, A.M., Dziewonski, A.M., and O'Connell, R.J., 1995. Thermal and chemical heterogeneity in the mantle: A seismic and geodynamic study of continental roots. *Phys. Earth Planet. Inter.*, 92: 45-55.
- Forte, A.M., and Mitrovica, J.X., 2001. Deep-mantle high-viscosity flow and thermochemical structure inferred from seismic and geodynamic data. *Nature*, 410: 1049-1056.
- Fuchs, K., Bonjer, K., Bock, G., Cornea, I., Radu, C., Enescu, D., Jianu, D., Nourescu, A., Merkler, G., Moldoveanu, T., and Tudorache, G., 1979. The Romanian earthquake of March 4, 1977. II. Aftershocks and migration of seismic activity. *Tectonophysics*, 53: 225-247.
- Girbacea, R., and Frisch, W., 1998. Slab in the wrong place: Lower lithospheric mantle delamination in the last stage of the Eastern Carpathian subduction retreat. *Geology* 26(7): 611-614.
- Goes, S., Govers, R., and Vacher, P., 2000. Shallow mantle temperatures under Europe from P and S wave tomography. *J. Geophys. Res.*, 105: 11,153-11,169.
- Green, D.H., and Falloon, T.J., 1998. Pyrolite: A Ringwood concept and its current expression. In: I. Jackson (Editor). *The Earth's Mantle*. Cambridge University Press, Cambridge: 311-378.
- Green, H.W. II, and Burnley, P.C., 1989. A new self-organizing mechanism for deep-focus earthquakes. *Nature*, 341: 733-737.

- Griffin, W.L., O'Reilly, S.Y., Ryan, C.G., Gaul, O., and Ionov, D.A., 1998. Secular variation in the composition of subcontinental lithospheric mantle: Geophysical and geodynamic implications. In: J. Braun et al. (Editors). *Structure and Evolution of the Australian Continent*. Am. Geophys. Union, Geodyn. Ser., 26: 1-26.
- Griggs, D.T., and Baker, D.W., 1969. The origin of deep-focus earthquakes. In: H. Mark and S. Fernbach (Editors). *Properties of Matter Under Unusual Conditions*. Wiley, New York: 23-42.
- Gutenberg, B., and Richter, C.F., 1954. *Seismicity of the Earth and Associated Phenomena*. Princeton University Press, Princeton, N.J., 2nd ed., 310 pp.
- Hacker, B.R., Peacock, S.M., Abers, G.A., and Holloway, S.D., 2003. Subduction factory. 2. Are intermediate-depth earthquakes in subducting slabs linked to metamorphic dehydration reactions? *J. Geophys. Res.*, 108: 2030, doi:10.1029/2001JB001129.
- Hackney, R., Martin, M., Ismail-Zadeh, A., Sperner, B., Ioane, D. and CALIXTO Working Group, 2002. The gravity effect of the subducted slab beneath the Vrancea region, Romania. In: J. Michalik, L. Simon and J. Vozar (Editors), *Proc. XVIIth Congress of the Carpathian-Balkan Geological Association*, Bratislava, September 1-4, 2002, *Geologica Carpathica*, 53: 119-121.
- Hammond, W.C., and Humphreys, E.D., 2000a. Upper mantle seismic wave velocity: Effects of realistic partial melt geometries. *J. Geophys. Res.*, 105: 10,975-10,986.
- Hammond, W.C., and Humphreys, E.D., 2000b. Upper mantle seismic wave velocity: Effects of realistic partial melt distribution. *J. Geophys. Res.*, 105: 10,987-10,999.
- Hauser, F., Raileanu, V., Fielitz, W., Bala, A., Prodehl, C., Polonic, G., and Schulze, A., 2001. VRANCEA99 – the crustal structure beneath the southeastern Carpathians and the Moesian Platform from a seismic refraction profile in Romania. *Tectonophysics*, 340: 233-256.
- Hauser, F., Prodehl, C., Landes, M., and the VRANCEA working group, 2002. Seismic experiments target earthquake-prone region in Romania. *EOS*, 83(41): 457, 462-463.
- Ioane, D., and Atanasiu, L., 1998. Gravimetric geoids and geophysical significances in Romania. In: D. Ioane (Editor). *Monograph of Southern Carpathians, Reports on Geodesy 7*, Institute of Geodesy and Geodetic Astronomy, Warsaw University of Technology, Warsaw, Poland: 157-175.
- Ismail-Zadeh, A.T., 2003. Modelling of stress and seismicity in the south-eastern Carpathians: Basis for seismic risk estimation. In: T. Beer and A.T. Ismail-Zadeh

- (Editors). Risk Science and Sustainability. Kluwer Academic Publishers, Dordrecht: 149-162.
- Ismail-Zadeh, A.T., Keilis-Borok, V.I., and Soloviev, A.A., 1999. Numerical modelling of earthquake flows in the southeastern Carpathians (Vrancea): Effect of a sinking slab. *Phys. Earth Planet. Inter.*, 111: 267-274.
- Ismail-Zadeh, A., Mueller, B., and Wenzel, F., 2003a. Modelling of descending slab evolution beneath the SE-Carpathians: implications for seismicity. In: F. Wenzel (Editor) *Challenges for Earth Sciences in the 21st Century*. Springer-Verlag, Heidelberg (accepted for publication).
- Ismail-Zadeh, A.T., Panza, G.F., and Naimark, B.M., 2000. Stress in the descending relic slab beneath the Vrancea region, Romania. *Pure Appl. Geophys.*, 157: 111-130.
- Ismail-Zadeh, A.T., Korotkii, A.I., Naimark, B.M., and Tsepelev, I.A., 2001. Numerical modelling of three-dimensional viscous flow under gravity and thermal effects. *Comput. Math. Math. Phys.*, 41(9): 1331-1345.
- Ismail-Zadeh, A.T., Andreescu, M., Demetrescu, C., Martin, M., and Wenzel, F., 2003b. Temperature structure beneath the southeastern Carpathians from seismic and heat flow data, submitted to *Tectonophysics*.
- Jaeger, J.C., and Cook, N.G.W., 1984. *Fundamentals of Rock Mechanics*. Chapman and Hall, London, New York, 3rd ed., 593 pp.
- Jiricek, R., 1979. Tectonic development of the Carpathian arc in the Oligocene and Neogene. In: M. Mahel (Editor). *Tectonic Profiles Through the Western Carpathians*, *Geol. Inst. Dionyz Stur*: 205-214.
- Jordan, T.H., 1979. Mineralogies, densities and seismic velocities of garnet lherzolites and their geophysical implications. In: F.R. Boyd and H.O.A. Meyer (Editors). *The Mantle Sample: Inclusions in Kimberlites and Other Volcanics*. Am. Geophys. Union, Washington, D.C.: 1-14.
- Karato, S., 1993. Importance of anelasticity in the interpretation of seismic tomography. *Geophys. Res. Lett.*, 20: 1623-1626.
- Karato, S., 2003. Mapping water content in the upper mantle. In: J. Eiler (Editor). *Subduction Factory*. Am. Geophys. Union, *Geophys. Monogr. Ser.*, in press.
- Kostrov, V.V., 1974. Seismic moment and energy of earthquakes, and seismic flow of rocks. *Izv. AN SSSR / Earth Phys.*, 1: 13-20.

- Krasovsky, S.S., 1989. Gravity Modeling of Deep-Seated Crustal Features and Isostasy (in Russian). Naukova Dumka, Kiev, 268 pp.
- Lenkey, L., Dovenyi, P., Horvath, F., and Cloetingh, S.A.P.L., 2002. Geothermics of the Pannonian basin and its bearing on the neotectonics. In: S.A.P.L. Cloetingh et al. (Editors). Neotectonics and Surface Processes: the Pannonian Basin and Alpine/Carpathian System. EGU Stephan Mueller Spec. Publ. Ser., 3: 29-40.
- Linzer, H.-G., 1996. Kinematics of retreating subduction along the Carpathian arc, Romania. *Geology*, 24: 167-170.
- Martin, M., Achauer, U., Kissling, E., Mocanu, V., Musacchio, G., Radulian, M., Wenzel, F. and CALIXTO Working Group, 2001. First results from the tomographic experiment CALIXTO'99 in Romania. *Geophys. Res. Abst.*, 3: SE1.02.
- Martin, M. and the CALIXTO working group, 2003. High resolution teleseismic P-wave tomography for SE-Romania. *Geophys. Res. Abst.*, 5: 10512.
- McKenzie, D.P., 1972. Active tectonics of the Mediterranean region. *Geophys. J. R. Astron. Soc.*, 30: 109-185.
- Mei, S., Bai, W., Hiraga, T., and Kohlstedt, D.L., 2002. Influence of melt on the creep behavior of olivine-basalt aggregates under hydrous conditions. *Earth Planet. Sci. Lett.*, 201: 491-507.
- Nitoi, E., Munteanu, M., Marincea, S., and Paraschivoiu, V., 2002. Magma-enclave interactions in the East Carpathian Subvolcanic Zone, Romania: petrogenetic implications. *J. Volcan. Geother. Res.*, 118: 229-259.
- Niu, Y., 1997. Mantle melting and melt extraction processes beneath ocean ridges: Evidence from abyssal peridotites. *J. Petrol.*, 38: 1047-1074.
- Oncescu, M.C., 1984. Deep structure of the Vrancea region, Romania, inferred from simultaneous inversion for hypocentres and 3-D velocity structure. *Ann. Geophys.*, 2: 23-28.
- Oncescu, M.C., and Bonjer, K.P., 1997. A note on the depth recurrence and strain release of large Vrancea earthquakes. *Tectonophysics*, 272: 291-302.

- Oncescu, M.C., and Trifu, C.I., 1987. Depth variation of moment tensor principal axes in Vrancea (Romania) seismic region. *Ann. Geophys.*, 5: 149-154.
- Radu, C., 1979. Catalogue of strong earthquakes occurred on the Romanian territory. Part I. – before 1901; Part II – 1901-1979 (in Romanian). In: I. Cornea and C. Radu (Editors). *Seismological Studies on the March 4, 1977 Earthquake*, Bucharest, Romanian: 723-752.
- Radu, C., 1991. Strong earthquakes occurred on the Romanian territory in the period 1901-1990 (in Romanian). *Vitralii*, 3: 12-13.
- Radulescu, F., Mocanu, V., Nacu, V., and Diaconescu, C., 1996. Study of recent crustal movements in Romania: a review. *J. Geodyn.*, 22: 33-50.
- Raleigh, C. B., and Paterson, M. S., 1965. Experimental deformation of serpentine and its tectonic consequences. *J. Geophys. Res.*, 70: 3965-3985.
- Sanders, C.A.E., Andriessen, P.A.M., and Cloetingh, S.A.P.L., 1999. Life cycle of the East Carpathian Orogen: erosion history of a doubly vergent critical wedge assessed by fission track thermochronology. *J. Geophys. Res.*, 104: 29,095–29,112.
- Sanders, C., Huisman, R., van Wees, J. D., and Andriessen, P., 2002. The Neogene history of the Transylvanian basin in relation to its surrounding mountains. In: S.A.P.L. Cloetingh et al. (Editors). *Neotectonics and Surface Processes: the Pannonian Basin and Alpine/Carpathian System*. EGU Stephan Mueller Spec. Publ. Ser., 3: 121-133.
- Schmidt, S., and Götze, H.-J., 1998. Interactive visualization and modification of 3D-models using GIS-functions. *Phys. Chem. Earth*, 23(3): 289-295.
- Sobolev, S.V., Zeyen, H., Stoll, G., Werling, F., Altherr, R., and Fuchs, K., 1996. Upper mantle temperatures from teleseismic tomography of French Massif Central including effects of composition, mineral reactions, anharmonicity, anelasticity and partial melt. *Earth Planet. Sci. Lett.*, 139: 147-163.
- Soloviev, A.A., and Ismail-Zadeh, A.T., 2003. Models of dynamics of block-and-fault systems. In: V.I. Keilis-Borok and A.A. Soloviev (Editors). *Nonlinear Dynamics of the Lithosphere and Earthquake Prediction*, Springer-Verlag, Heidelberg: 69-138.
- Sperner, B., Lorenz, F., Bonjer, K., Hettel, S., Müller, B., and Wenzel, F., 2001. Slab break-off – abrupt cut or gradual detachment? New insights from the Vrancea region (SE Carpathians, Romania). *Terra Nova*, 13: 172-179.

- Smith, G.P., Wiens, D.A., Fischer, K.M., Dorman, L.M., Webb, S.C. and Hildebrand, J.A., 2001. A complex pattern of mantle flow in the Lau backarc. *Science*, 292: 713-716.
- Stein, R., 1999. The role of stress transfer in earthquake occurrence. *Nature*, 402: 605-609.
- Takei, Y., 2000. Acoustic properties of partially molten media studied on a simple binary system with a controllable dihedral angle. *J. Geophys. Res.*, 105: 16,665-16,682.
- Trushkov, V.V., 2002. An example of (3+1)-dimensional integrable system. *Acta Applicandae Mathematicae*, 72(1-2): 111-122.
- Wenzel, F., Lorenz, F.P., Sperner, B., and Oncescu, M.C., 1999. Seismotectonics of the Romanian Vrancea area. In: F. Wenzel, D. Lungu and O. Novak (Editors). *Vrancea Earthquakes: Tectonics, Hazard and Risk Mitigation*. Kluwer Publishers, Dordrecht: 15-25.
- Wortel, M.J.R., and Spakman, W., 2000. Subduction and slab detachment in the Mediterranean-Carpathian region. *Science*, 290: 1910-1917.
- Zugravescu, D., Polonic, G., Horomnea, M., and Dragomir, V., 1998. Recent vertical crustal movements on the Romanian territory, major tectonic compartments and their relative dynamics. *Rev. Roum. de Geophysique*, 42: 3-14.

Tables

Table 1. Laterally averaged compressional seismic wave velocities (v_p), density (ρ_*) calculated from v_p , and average temperature (T_*).

Depth, km	v_p , km s ⁻¹ (1)	ρ_* , 10 ³ kg m ⁻³ (2)	T_* , °C (3)
0	2.7	1.59	20
2.5	3.5	1.84	80
5.0	4.5	2.17	130
7.5	5.2	2.39	180
10.0	5.7	2.55	230
12.5	5.8	2.58	290
15.0	5.9	2.61	350
20.0	6.2	2.71	420
25.0	6.7	2.87	510
30.0	6.9	2.94	600
35.0	7.0	2.97	670
40.0	8.0	3.28	740
50.0	8.1	3.32	820

(1) Hauser et al, 2001, 2002

(2) Krasovsky, 1989

(3) Demetrescu and Andreescu, 1994

Table 2. Model parameters

Background crustal density	Fig. 3 and Table 1
Background mantle density	Fig. 3
Background crustal viscosity	10 ²³ Pa s
Background mantle viscosity	10 ²⁰ Pa s
Background slab viscosity	10 ²² Pa s
Background temperature	Fig. 3
Coefficient of thermal expansion, α	3×10 ⁻⁵ K ⁻¹
Activation energy, E	5×10 ⁵ J mol ⁻¹
Activation volume, V	2×10 ⁻⁵ m ³ mol ⁻¹
Universal gas constant, R	8.3 J mol ⁻¹ K ⁻¹
Acceleration due to gravity, g	9.8 m s ⁻²
Vertical size of the model, l_3	350 km
Horizontal sizes of the model, l_1 and l_2	1050 km
Stress scale	4×10 ⁴ MPa

Figure captions

Fig. 1. Observed seismicity in Romania for the last decade with magnitude $M_w \geq 3$ (after Oncescu and Bonjer, 1997; Sperner et al., 2001). (a) Epicenters of Vrancea earthquakes determined by the joint hypocenter method. The background is the topography; the two bold lines show the location of the refraction seismic profiles VRANCEA99 (N-S) and VRANCEA2001 (E-W). (b) Hypocentres of the same earthquakes projected onto the NW-SE vertical plane AB (dashed line in (a)). DO, Dobrogea orogen; EEP, Eastern European platform; MP, Moesian platform; and TB, Transylvanian basin.

Fig. 2. Seismic tomographic image of the Vrancea slab (Martin et al., 2001) and hypocenters of earthquakes (circles and asterisks indicate the location and magnitude of seismic events). Three shaded grey surfaces represent the surfaces of 1%, 1.5%, and 2% positive anomalies of P-wave velocity obtained via teleseismic data inversion. The top surface illustrates the topography. Focal spheres are fault plane solutions for the four largest Vrancea intermediate-depth earthquakes in the XXth century.

Fig. 3. Density and temperature versus depth used as the background parameters in the modeling. Density curve: the laterally averaged density obtained from the P-wave velocity to density relationship (Krasovsky, 1989) for the 50-km upper layer of the model (shaded zone) and the density derived from PREM for the rest of the model domain. Temperature curve: the laterally averaged temperature (Demetrescu and Andreescu, 1994).

Fig. 4. Temperatures derived from P-wave velocity anomalies beneath the SE-Carpathians at different depths in the mantle. The composition, anharmonicity, anelasticity, and partial melting are taken into account. Isolines present the surface topography. Red star shows the location of the Vrancea intermediate-depth earthquakes.

Fig. 5. Temperature in the crust (left; after Demetrescu and Andreescu, 1994) and subcrustal mantle (right; Demetrescu and Andreescu, unpublished data) estimated from the surface heat flux in the region. Isolines present the surface topography. Black star shows the location of the Vrancea intermediate-depth earthquakes.

Fig. 6. Predicted contemporary flow induced by the descending slab beneath the SE-Carpathians. Blue and orange cones illustrate downward and upward flow, respectively. The violet surface in the middle of the model domain is the surface of 2%

positive P-wave velocity anomaly (modeled slab). The top surface is the topography. Red and blue arrows on the top of the surface topography are GPS data on the vertical movements in the Vrancea region (Dinter et al., 2001). Circles ($M_w < 6.5$) and asterisks ($M_w > 6.5$) mark the hypocenters of the Vrancea earthquakes.

Fig. 7. Map of predicted uplift and subsidence in the SE-Carpathians at 15 km depth. White and black dots illustrate the relative vertical movements at the surface as derived from GPS measurements (Dinter et al., 2001). Isolines present the surface topography. DO, Dobrogea orogen; EEP, Eastern European platform; FB, Foscani basin; MP, Moesian platform; and TB, Transylvanian basin.

Fig. 8. Comparison of the location of positive P-wave velocity anomalies, earthquake hypocenters, and predicted maximum shear stress. Upper panel: NW-SE seismic tomography cross-section through the SE-Carpathian region (after Martin et al., 2001) and the projection onto this cross-section of the hypocenters of the Vrancea earthquakes from the last decade. Lower panel: predicted maximum shear stress for the same cross-section. The dashed boxes delineate the area of hypocenters and maximum shear stress.

Fig. 9. Maximum shear stress beneath the SE-Carpathians at different mantle depths. Isolines present the surface topography. Black star marks the location of the Vrancea intermediate-depth earthquakes.

Fig. 10. Maximum horizontal stress (compression is positive and tension is negative) beneath the SE-Carpathians at different mantle depths. Isolines present the surface topography. Black star marks the location of the Vrancea intermediate-depth earthquakes.

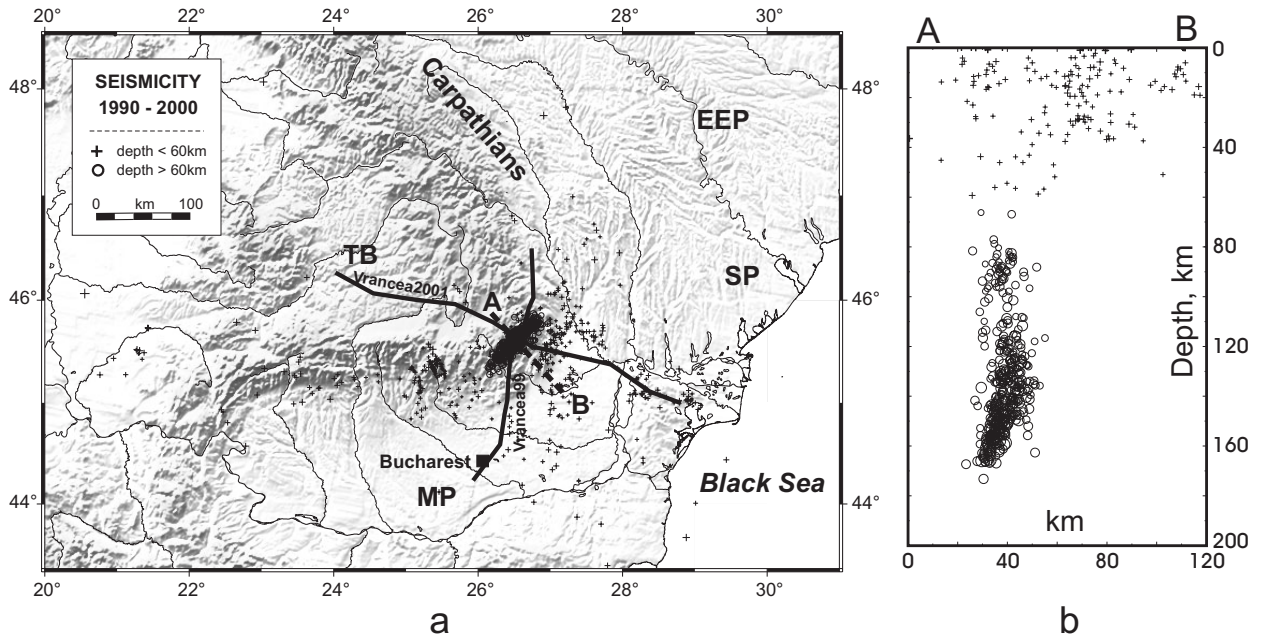


Fig. 1

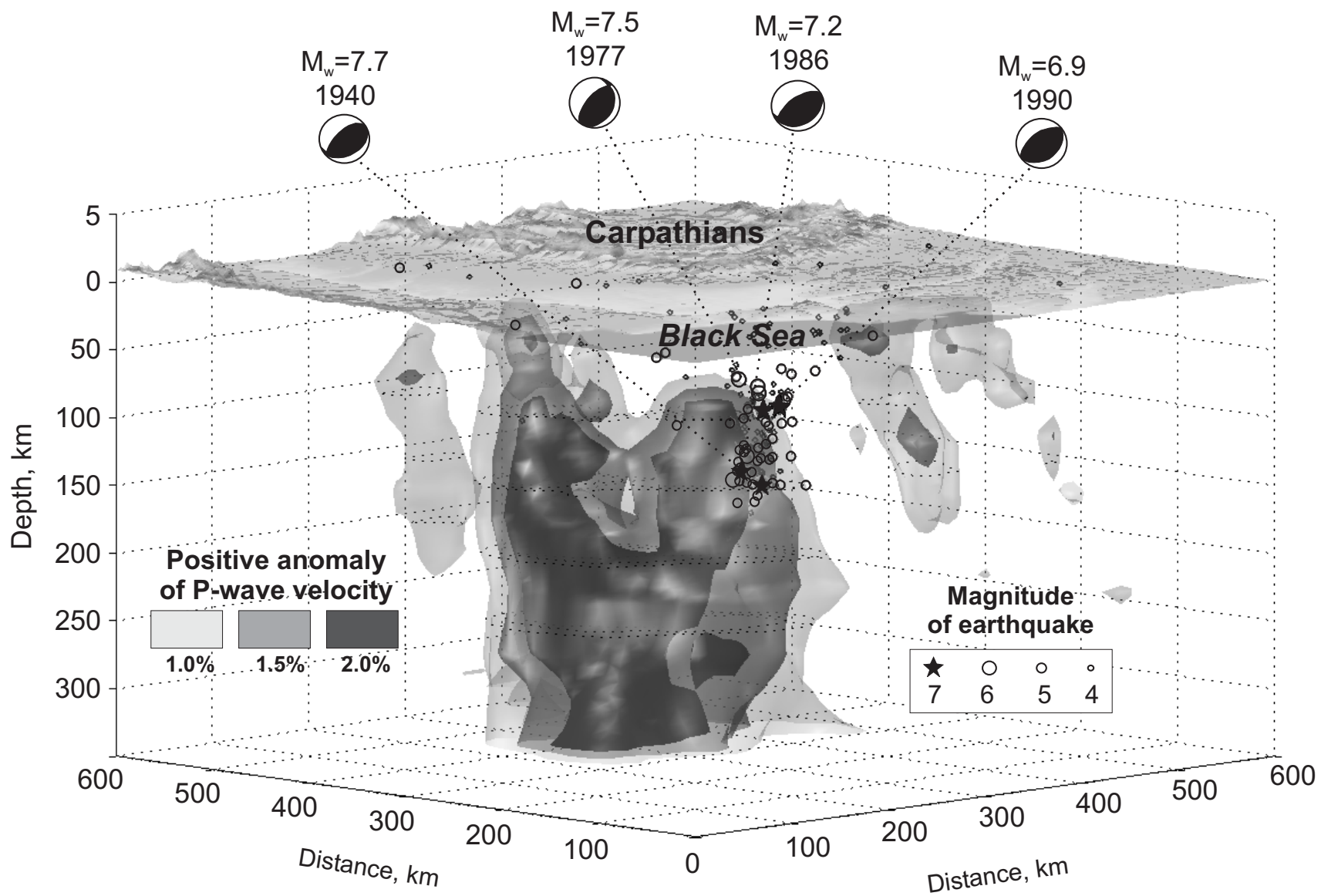


Fig. 2

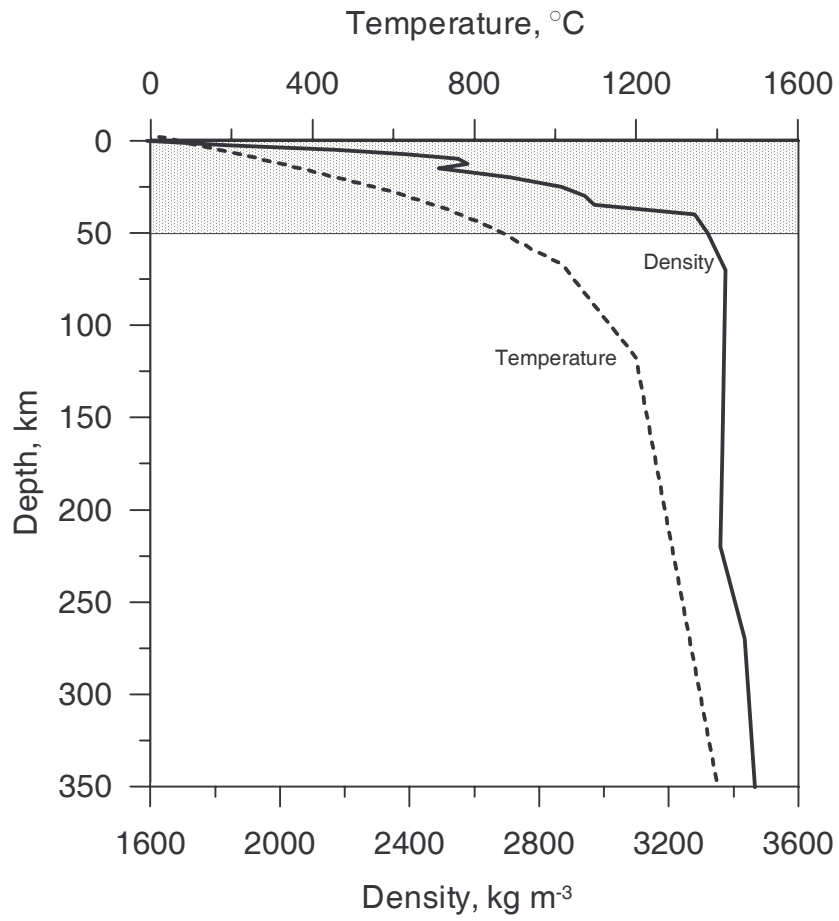


Fig. 3

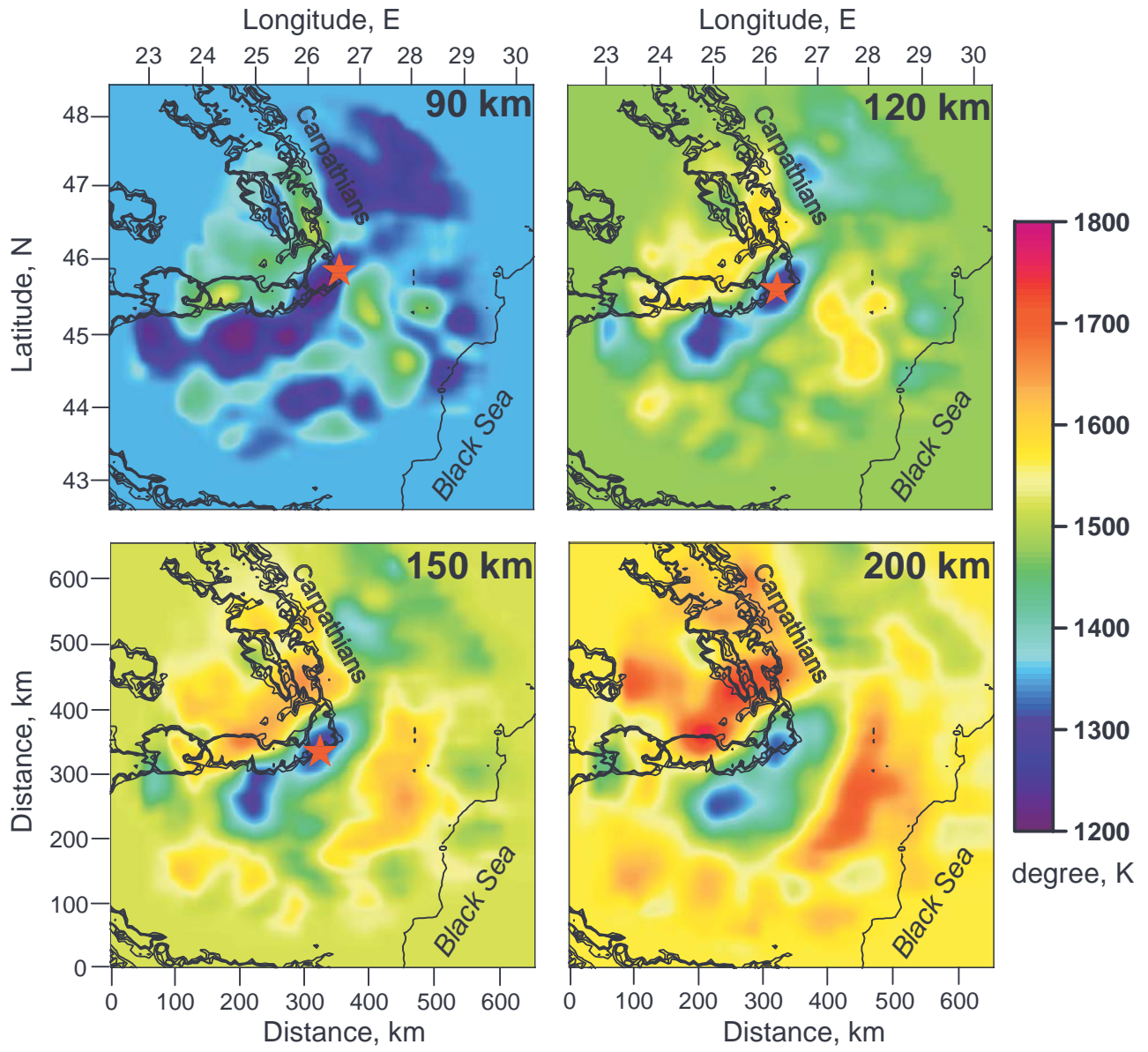


Fig. 4

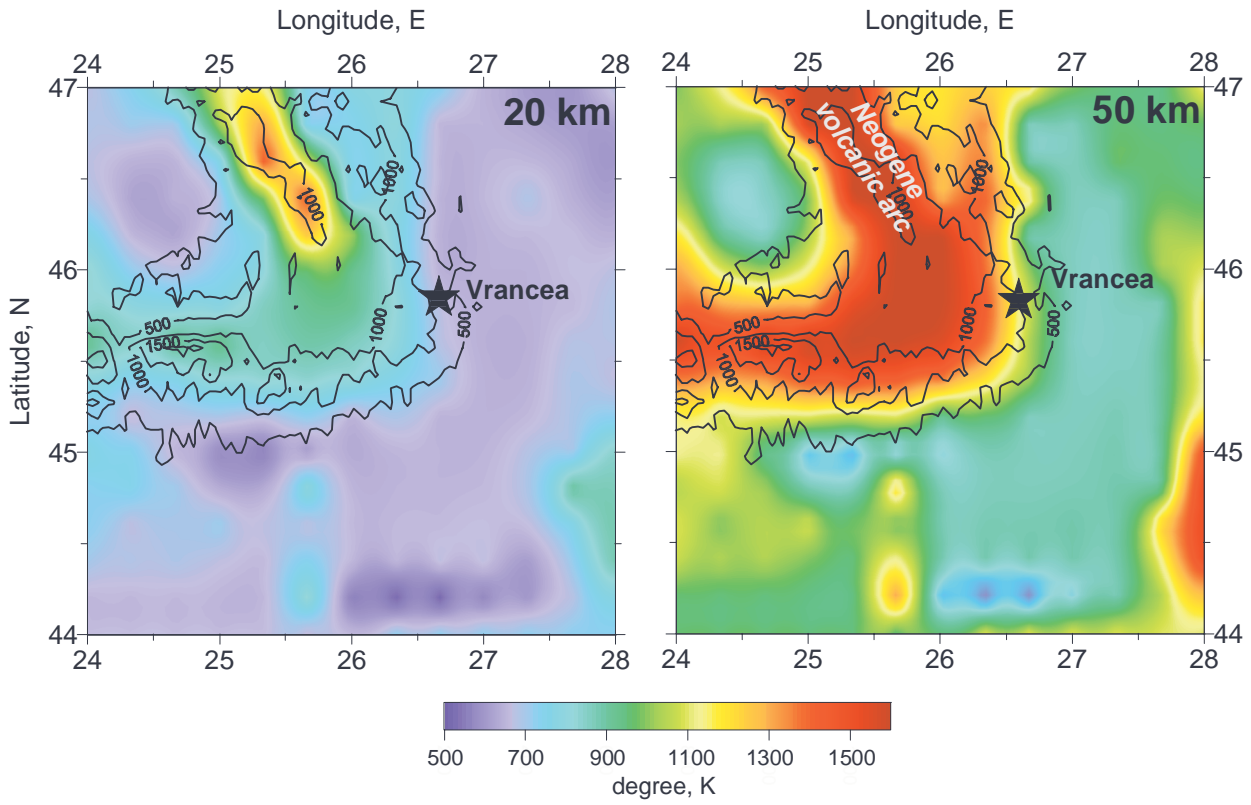


Fig. 5

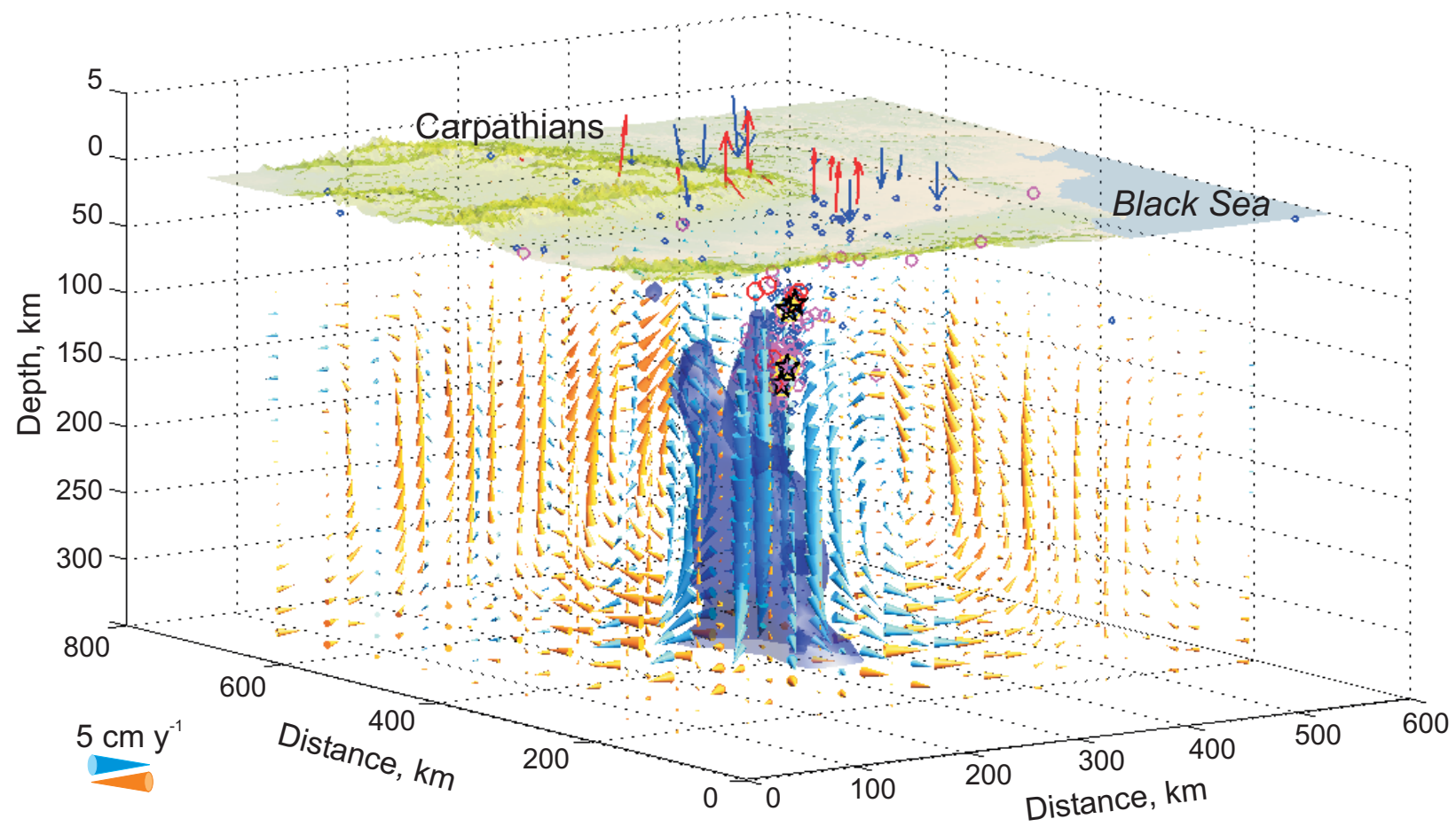


Fig. 6

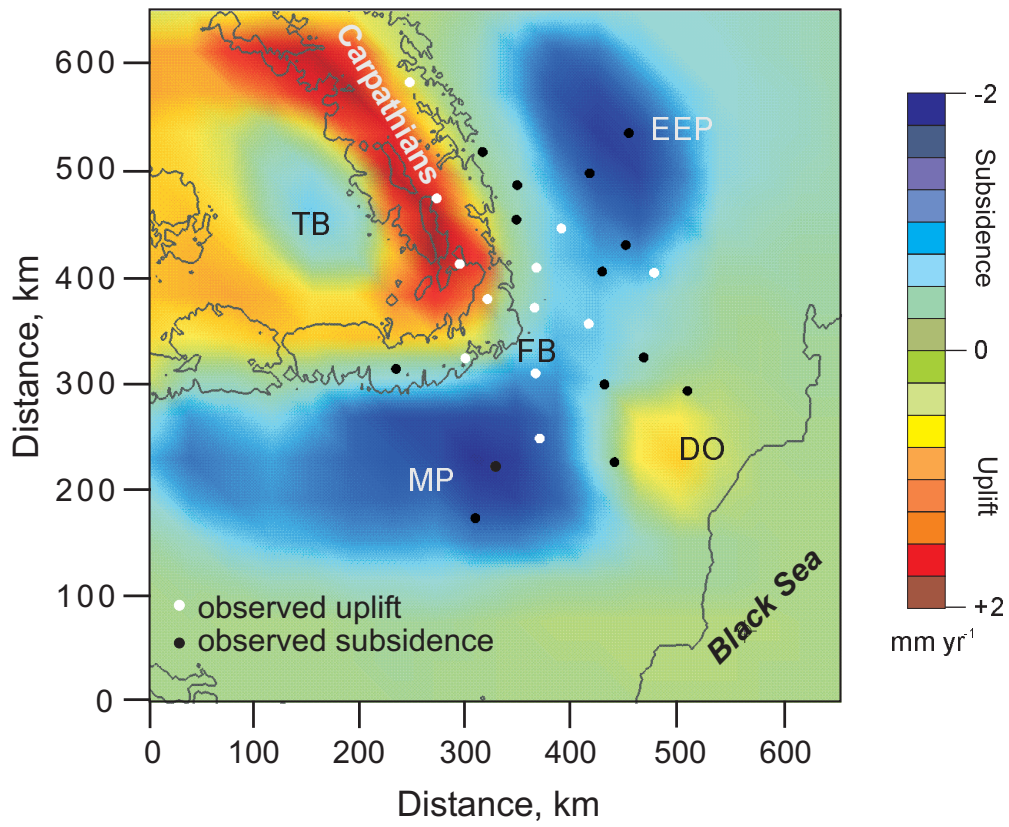


Fig. 7

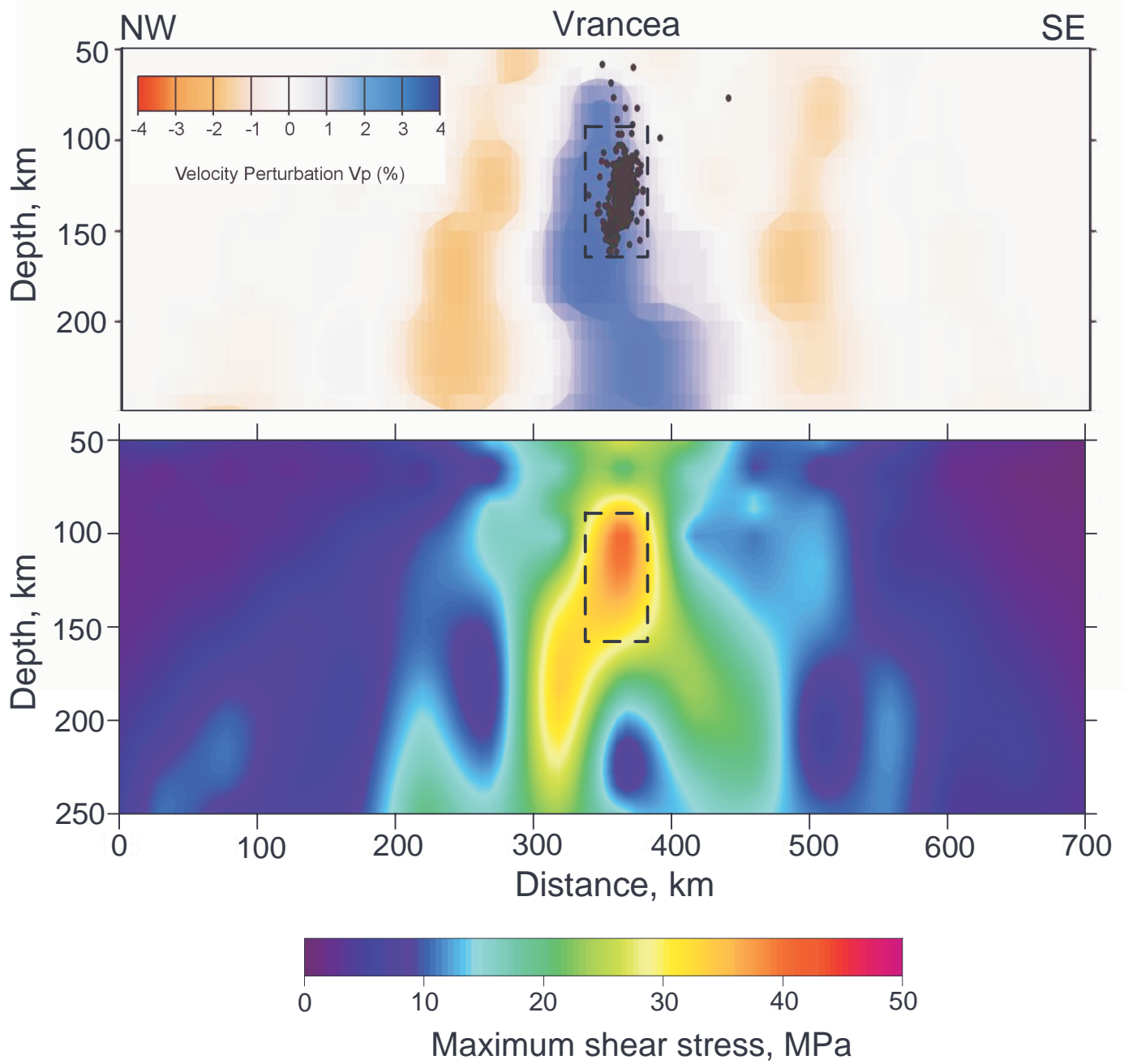


Fig. 8

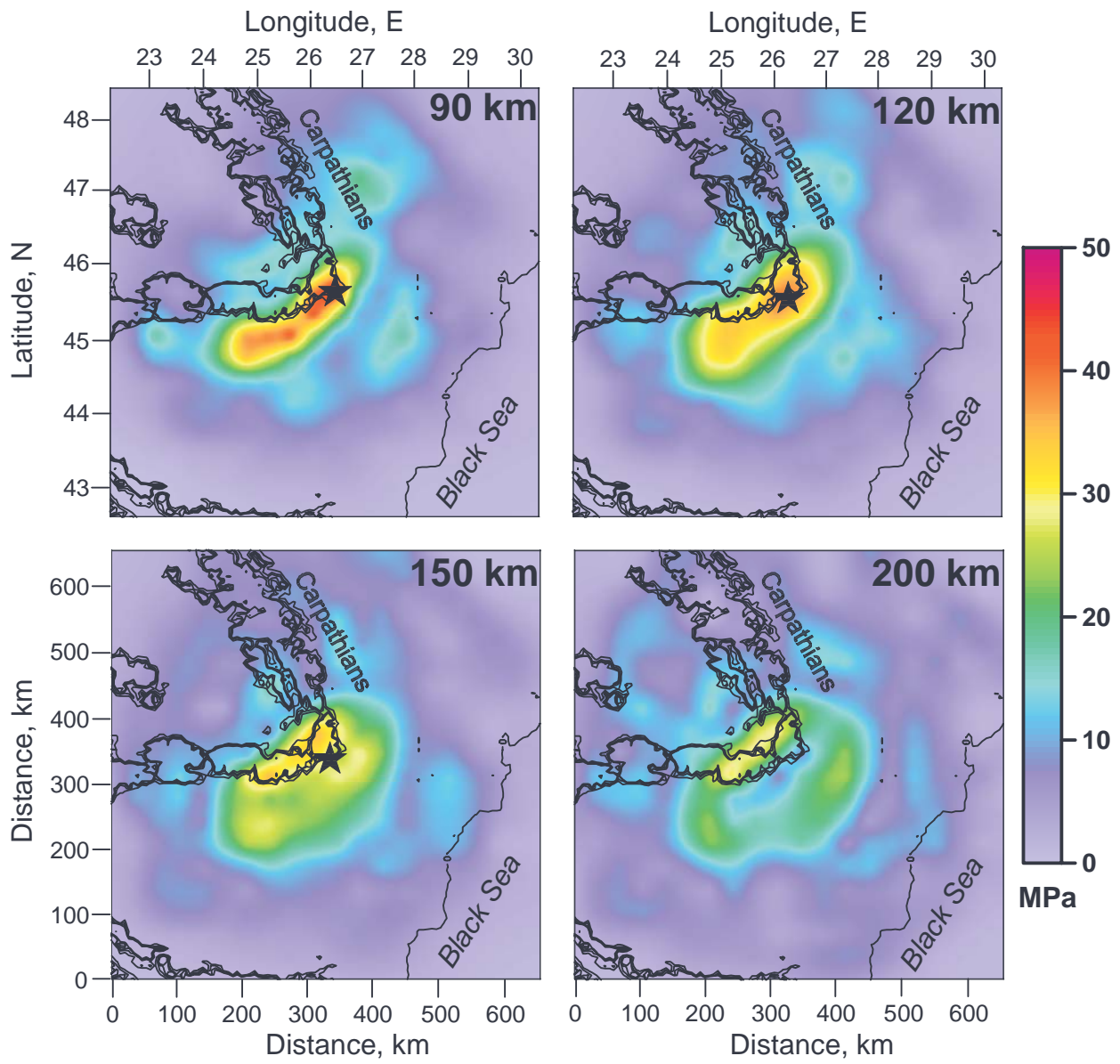


Fig. 9

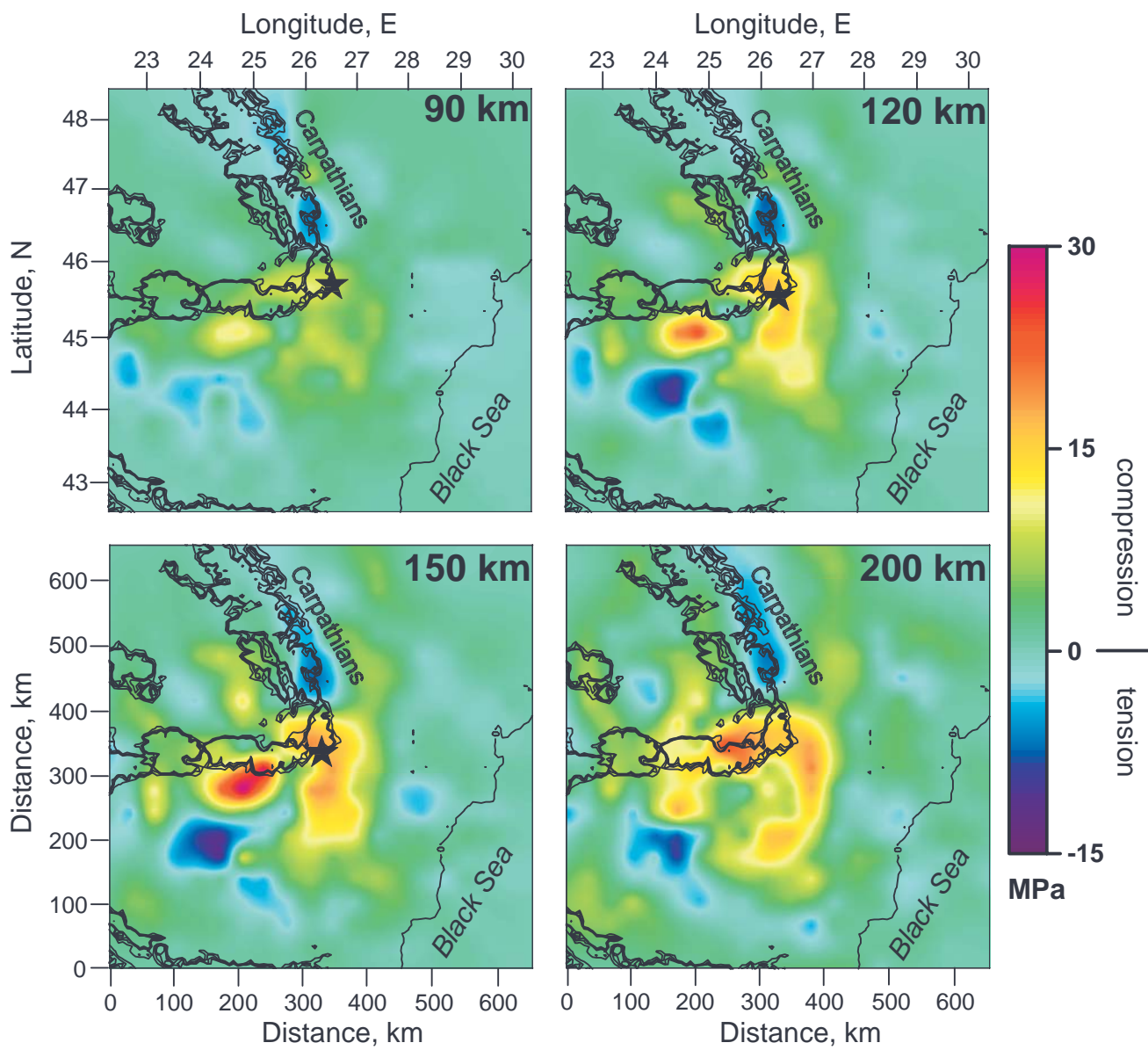


Fig. 10